Divergence-Free Fields in the Solution of Waveguide Problems by Finite Elements

by

Allan John Kobelansky
B. Eng. (Electrical)

A thesis submitted to the Faculty of Graduate Studies and Research
in partial fulfillment of the requirements for the degree of
Master of Engineering

Department of Electrical Engineering
McGill University
Montreal, Canada
September, 1988

Abstract

Spurious solutions in the finite-element analysis of the modes of waveguides are completely eliminated by the use of fields which are exactly divergence-free. The solenoidal fields are themselves computed by the finite-element method.

The technique, known as the *Reduction Method*, is related to the much used *Penalty Method*. The premise of the method is to use divergence-free trial functions which are generated by solving an alternate functional; the zero-valued stationary points of which correspond to fields which are divergence-free. These fields are then used as trial functions in the classical curl-curl functional. Stationary points of this functional correspond to the true modes of the waveguide.

The method is applied to empty and dielectric loaded waveguides.

Sommaire

L'usage de champs exactement non-divergents élimine complètement les solutions sporadiques attribuables à l'utilisation de la méthode de calcul par éléments finis dans le calcul des modes de guides d'ondes. Ces champs exactement non-divergents (de nature solénoïdale) sont eux-mêmes obtenus par le biais de la méthode de calcul par éléments finis.

La technique utilisée, connue sous le nom de *Méthode Réductionnelle*, s'apparente à la *Méthode du Coût* (*Penalty Method*) dont l'usage est plus répandu. La technique réductionnelle est basée sur l'utilisation de fonctions d'essai non-divergentes générées en résolvant une autre fonctionnelle dont les points stationnaires à valeur nulle correspondent aux champs non-divergents. Ces champs sont par la suite utilisés comme fonctions d'essai dans la fonctionnelle "rotationel-rotationel" classique. Les points stationnaires de cette fonctionelle correspondent aux modes réels du guide d'ondes.

Cette méthode est appliquée à des guides d'ondes vides et contenant un matéraux diélectrique.

Acknowledgements

There are many people I would like to thank for contributing either directly or indirectly to this thesis. I would like to thank Dr. Geoff Stone for introducing me to finite-elements during the summer of '83. Dr. Pete Silvester was kind enough to hire me as a research assistant in his lab and provided me with much needed financial assistance. The mere presence of Dr. Silvester was enough to inspire anyone to learn electromagnetics. Dr. Dave Lowther was the source of much of my software engineering skills acquired during my formative years. For that I am very grateful.

Graduate school would not have been a reality were it not for the support and encouragement of my thesis supervisor, Dr. Jon Webb. Jon made what some people would consider a mundane topic, interesting and exciting. I am very proud to have been associated with Jon. He made me accomplish things I never would have dreamed possible.

The quality of students I had the opportunity to work with was outstanding. People like, Nevine Nassif, Robert Kotuiga, Jean-Francois Ostiguy, Steven Fraser, Steve McFee, Amy Pinchuck, Sean Marrett, Munna Mishra, Chris Crowley, Toufic Boubz, and Andy Froncioni. Andy was the primary motivator that got me started and kept me going until this thesis was finally completed. I apologize to those whose names I have left out. To all of you, thanks.

Needless to say, my family played an important role in making it possible for

me to attend university in the first place. To my parents, John and Gisele, my sister, Diane, I hope I've made you proud.

Many thanks to Dave Bernardi for translating the abstract into french, and to Robert Blumenthal for his TEXpertise.

To Mrs. Peggy Hyland, I told you I would finally submit!

Contents

List of Figures

List of Tables

Chapter 1

Introduction

1.1 Background

For a little over 50 years, researchers have been analysing the properties of waveguide structures using a myriad of techniques and rules of thumb. Beyond trivial waveguide structures, analytical solutions become increasingly difficult to generate. For this reason, numerical methods were developed to assist the engineer in the analysis of these waveguides. In light of the widespread use of Computer Aided Design and Analysis techniques, an ideal scenario would envision the design of an arbitrary waveguide with user-definable materials and boundary conditions. The benefits of such a system would be enormous. The results of the numerical analysis would serve as a guideline in the manufacturing process and remove much of the guesswork

in designing waveguides and resonant cavities.

The goal of this paper is to present a method for designing and analysing dielectric loaded waveguides suitable for implementation on a computer. The method consists of a variational principle based on the finite element method. A feature of this method is the suppression of so called spurious modes often encountered in the solution of eigenvalue problems. This is accomplished by employing divergence free basis vectors in the solution of the boundary value problem. As a result of this work, a completely general finite element program is developed which assumes nothing about the basis vectors being used. How the divergence free basis vectors are computed and how they are used is the subject of this research.

1.2 Historical context

Much work has been done to analyze waveguide structures in general. In 1936, W.L. Barrow[1] published a paper declaring that electromagnetic energy could be transmitted through the inside of hollow tubes of metal, provided the frequency of transmission was greater than a certain critical value.[1] This value, known as the it cutoff frequency, below which no transmission is possible is probably the most important waveguide characteristic. Much

[1]Southwark and Carson, Mead and Schelkunoff published similar work in April, 1936. Lord Rayleigh's paper "On passage of electric waves through tubes ...", Phil. Mag., 43 (1897) p.125, was the first paper on the subject.

research has been done in order to find this and other waveguide parameters both practically and analytically.

1.3 Previous works

In 1956 A.D. Berk[2] published a paper that presented a variational principle for waveguide structures. It was around this variational formulation that much work subsequently evolved. Several modifications to the variational formulation were possible to yield an E-field, H-field, or mixed-field solution. The pure H-field formulation proved to be the choice of many.

In 1968, S. Ahmed[3] recognized the usefulness of the finite-element method as an analytical tool and presented a variational formulation for waveguide problems. Although his variational formulation did not resemble Berk's it did introduce some fundamental ideas that are still in use today. His method, based on a scalar functional, was inadequate for the inherently hybrid modes encountered in inhomogeneous or anisotropic problems.

In 1969, P.P. Silvester[4] presented a general finite element waveguide analysis program based on a variational formulation that used a functional which had as its corresponding Euler equation, the Helmholtz equation. In this paper, Silvester analyzed empty waveguide structures exclusively yet recognized that this general approach would equally be suited to inhomogeneously filled guides and cavity resonators. This one component method

worked well for two-dimensional waveguides, but like Ahmed's method was inadequate for hybrid mode waveguides.

Later that same year, S. Ahmed and P. Daly[6] presented finite-element methods for inhomogeneous waveguides. For the first time modes were encountered which had no physical significance. The authors attributed these *spurious modes* to the numerical method. The method used an axial component of the fields E_z-H_z, which without destroying the canonical form of the eigenvalue matrix, could not treat general anisotropic problems. For waveguides with arbitrary dielectric distribution, satisfying the boundary conditions proved to be quite difficult.

In 1970, Z.J. Csendes and P.P. Silvester[7] proposed a numerical solution of dielectric loaded waveguides based on the finite element method. Their variational formulation was based on the so called E_z-H_z formulation of the Helmholtz equation. Like their predecessors, they obtained non-physical modes that were attributed to the numerical technique. The authors claimed that although these modes could not be eliminated mathematically, they could be detected by their non-physical behavior. They suggested a tedious at best method of plotting the fields and recognizing those plots which "did not appear nice". Clearly this method was limited.

P. Daly[8] in 1971 introduced a hybrid-mode analysis of microstrip technique similar to those used previously for waveguide structures. His difficulty was dealing with a singularity in a matrix produced by the variational formulation's inability to cope with inhomogeneity in the guide. Spurious modes

were produced as a result, in the region of the singularity.

In 1972, D.G. Corr and J.B. Davies[10] developed a computer analysis of the fundamental and higher order modes in single and coupled microstrip based on a finite difference technique using a variational formulation. They too encountered spurious modes and believed that their existence was due to the "indefinite nature of the variational expression". They recognized that spurious modes were related to an excess of degrees of freedom in the problem. They reported that spurious modes only occurred for an indefinite system and not for a definite system. They also observed that there was a one to one correspondence between the number of free boundary points and the number of spurious solutions.

In 1974, C.G. Williams and G.K. Cambrell[11] used transverse field components to analyse surface waveguide modes. Their technique did not yield spurious solutions but any light shed by their work was not applicable to closed waveguide structures. Variational formulations using transverse field components solved by the Raleigh-Ritz method do not produce spurious modes, but unfortunately lack applicability to problems with anisotropic materials. The functionals were not self adjoint, and because of the added differentiation involved with them, were not very attractive for a finite-element implementation. The non-appearance of spurious solutions in this formulation was most likely due to the divergence-free basis functions used.

That same year M. Albani and P. Bernardi[12] introduced a numerical method for finding the modes inside resonant cavities and waveguides of

arbitrary shape, based on the discretization of Maxwell's equations in integral form. The method was straightforward in it's implementation; the problem was discretized into cells and for each cell Maxwell's equations were directly applied. Their method apparently produced no spurious modes although this fact was not explicitly stated. It proved to be an interesting approach but unfortunately did not offer the generality and flexibility of the finite element method.

A novel approach developed by S. Akhtarzad and P.B. Johns[13] in 1975 using the transmission-line matrix method was proposed offering versatility and generality offered by no other method of that period. This method assumed that internodal connections could be made with generalized transmission line properties. It was conceptually simple but for relatively simple cases and beyond, the intuitive nature of the problem got shrouded in details. For an experienced microwave engineer this method was useful and effective. As the basis of a Computer Aided Design package this method demanded too much knowledge on behalf of the operator.

In 1975, C. Yeh, S.B. Dong and W. Oliver[14] proposed a method by which the propagation characteristics of optical fibres could be studied. Unlike waveguide structures of interest in this thesis, optical waveguide problems possess infinite boundaries and as such the method proposed goes to great lengths to provide for this. According to the authors, their method worked well for arbitrarily complex guiding structures and the results agreed well with those computed previously by other authors. No mention was made of

spurious modes.

In 1976 A. Konrad[15] published a vector variational formulation of electromagnetic fields in anisotropic media. Konrad's work used a full three component H-field formulation. Konrad made full mention of previous work regarding spurious modes and stated that these modes were caused by a larger than expected set of natural boundary conditions. His proposed method also introduced spurious modes but he claimed that they were predictable and unique solutions which did not satisfy the electromagnetic boundary conditions at perfect conductors. He proposed imposing more boundary conditions as a cure for eliminating the spurious modes.

That same year P. Vandenbulke and P.E. Lagasse[16] used the finite-element method with a variational formulation to perform an eigenmode analysis of anisotropic optical fibres. Although no mention was made about spurious modes, a subsequent paper admitted to the difficulty arising in using this same technique.

In 1977, Konrad[17] published a high-order triangular finite element method for electromagnetic waves in anisotropic media. The method had many advantages over his previous work, most notably increased accuracy, yet suffered from spurious modes as was the case previously. One advantage of this method was it's usefulness in dealing with isotropic and anisotropic media.

T.S. Bird[18] encountered spurious modes using a hybrid finite-element technique to determine the propagation and radiation characteristics of rib

waveguides. He used several differing discretizations to track the true modes since he noticed that spurious modes were unstable in their occurrence in the spectrum.

In 1978 T.G. Mihran[20] tried to develop corporate interest in developing a generalized method for analysing microwave devices. He stressed the rapidly growing commercial importance of microwave ovens and the empirical nature of their design. His paper was concerned about tuning microwave ovens and he suggested further work to be done to develop a general method to analyze these devices.

R.L. Ferrari and G.L. Maile[21] presented a full three component vector variational formulation for solving electromagnetic problems. Their paper was specifically addressed at finding the dominant-mode resonant frequencies for two cases of dielectric loaded waveguides. Spurious modes did not pose a problem for them since the dominant modes were easily recognized.

In 1981, N. Mabaya, P.E. Lagasse, and P. Vandenbulke[22] submitted a finite element program for the analysis of anisotropic optical waveguides. It is in this paper that the authors admitted to spurious modes obtained previously. They suggested for the first time that the spurious modes may be caused by the non-positive definiteness of the functional. They stated that in general, locating the first true mode was simple since it corresponded to the first positive eigenvalue in the solution. They supported this argument by stating that a plot of other modes revealed unnatural variations in the cross section. They admitted that determining higher modes posed a

greater problem. A noteworthy mention in this paper was that the number of spurious modes is reduced by strictly enforcing continuity of the tangential components of the transversal fields, at the interfaces, by means of Lagrange multipliers. Their two scalar formulations E-H and H-E, yielded no spurious modes and this was attributed to the positive definiteness of the functionals.

M. Ikeuchi, H. Sawami and H. Niki[23] developed a variational finite-element formulation for open-type dielectric waveguides. Modifications pertinent to their functional were required to take care of open boundaries. They too encountered spurious modes that behaved like physical modes further complicating the analysis.

In 1982, M. Koshiba, K. Hayata, and M. Suzuki[24] extended work done by Mabaya *et al*[22] to include the analysis of anisotropic optical waveguides with a diagonal permittivity tensor. Their method produced no spurious modes but offered little to the analysis of closed waveguide structures.

J.B. Davies, G.Y. Philippou and F.A. Fernandez[27] published a paper on the analysis of all modes in cavities with circular symmetry. This paper presented the most complete analysis of spurious modes to date. Several observations were made about spurious modes: the infinite multiplicity of the zero eigenvalue was believed to be the major cause of trouble. They also suggested that boundary conditions be rigorously enforced. Their findings indicated that spurious solutions have a non-zero divergence in the region. Unfortunately, imposing more boundary conditions did not eliminate all spurious modes.

In 1983, K. Gustafson and R. Hartman[29] suggested a way to compute divergence-free bases for finite element methods in hydrodynamics. The application to waveguides was not trivial but their method implied that trial functions may by computed a *priori* and that these trial functions would satisfy the non-divergence nature of solutions of waveguide problems.

Later that year, M. Hara, T. Wada, T. Fukasawa and F. Kikuchi[31] produced a paper which took the zero-divergence issue at hand and imposed a penalty term that explicitly penalized divergent solutions. This had the effect of pushing the undesirable solutions out of the spectrum of interest, but not eliminating them. Their method imposed severe restrictions on the cavity shapes that could be analysed, and only works on empty waveguide cavities.

In 1984 M. Hano[34] introduced a method using a variational formulation with a conforming element. The method did not produce any spurious modes but did produce many needless zero modes. The usefulness of this method was restricted to rectangular guides since the conforming element was rectangular. His method did not enforce constant permeability or permittivity throughout the region as did Konrad's method.

M. Koshiba, K. Hayata, and M. Suzuki[33] presented a method reminiscent of the penalty method in which divergent terms were penalized. They claimed no spurious modes in this vector-variational approach whereas in fact an implementation of their work revealed that undesirable modes were simply pushed up and out of the range of frequencies of interest. Their method

did not reduce the size of the matrix problem, an underlying theme in many papers of the day.

One month later these same authors published[32] a scalar finite-element analysis of anisotropic optical waveguides with off-diagonal elements in a permittivity tensor. There method did not produce spurious modes, but then again, the method was only approximate.

B.M.A. Rahman and J.B. Davies[35] produced a vector variational formulation for analysing optical and microwave waveguide problems. Like other workers of their time they too encountered spurious modes. As was mentioned in their paper their exact cause was still the very debatable. They did however develop a method to specify the probability of a solution being real or spurious. A physical eigenvector would satisfy the zero divergence condition whereas spurious modes would not. In practice the true solutions had much less divergence values than did the spurious solutions. They attempted to pinpoint the source of the spurious modes on, the lack of enforcement of the boundary conditions, the positive definiteness of the operator, and also on the non-divergence of the trial functions making the system too flexible. They imposed more boundary conditions than usual but spurious modes still appeared.

Rahman and Davies[36], presented a more formal approach to the penalty method used previously. They included a lengthy discussion about spurious modes and their existence. Their work indicated that spurious modes were caused by systems which were too flexible. They observed that spu-

rious modes did not appear in a scalar formulation because the operator was positive definite, in contrast with a vector finite element method where the operator was no longer positive definite. They suggested that spurious modes could be identified by examination of their dispersion curves. They also suggested that the eigenvectors be plotted since a non-physical mode varied in an unreasonable way, and so those fields which varied unreasonably could be identified as being spurious. Spurious modes could also be tracked by observing the convergence of the solutions with mesh refinements. It was also recognized that the divergence of the spurious modes was very high.

The year 1985 saw several papers using finite-element techniques to analyse waveguide structures. D. Welt and J.P. Webb[39] described a method using a functional approach with a curvilinear element. They too obtained spurious modes which were eliminated by plotting the resulting field solutions.

J.P. Webb[41] later published a paper using the penalty method for finding the modes of dielectric loaded cavities. He correctly identified that there was an infinity of solutions corresponding to the zero eigenvalue and that this was the cause of the spurious modes.

R.B. Wu and C.H. Chen[40] used a variational reaction theory for analysing dielectric waveguides. They did not seem to get spurious modes but the implementation of their method was not general enough for a computer-aided environment.

Konrad[42] published a direct three-dimensional finite element method for the solution of electromagnetic fields in cavities. His method attempted to impose the non-divergence of the solutions by imposing $\nabla \cdot \mathbf{H} = 0$ directly. The method worked correctly by eliminating degrees of freedom and thus made the system more rigid. However, it was only demonstrated for one element geometries.

He reduced the problem size by taking advantage of symmetry wherever possible and applying appropriate boundary conditions. His method looked promising but until then only worked for one element models.

K. Hayata *et al* [44] published a vectorial finite-element method using transverse magnetic-field components that did not yield any spurious modes. Their technique was to impose the zero divergence condition implicitly, by rewriting the divergence-free constraint in terms of the z-component of the **H** field. This in turn is substituted into the original matrix formulation. The drawback of this method is the explicit division by the phase constant β which causes the matrices to blow up when β approaches zero.

Recently, C. W. Crowley [45] introduced the notion of using covariant projection elements for 3D vector field problems. This paper states that with a suitable modeling of the geometry with these covariant elements, spurious-free solutions may be generated. The advantages of this method are many. No penalty terms or global constraints are required. In addition, scalar methods may be extended directly to vector methods, without special modifications. The disadvantage of this method is that the spurious modes

are not eliminated. The method simply assures that the spurious modes will have zero eigenvalues. There is little savings here since the spurious modes must still be computed.

J.P. Webb [46] used a modified penalty method which allows for a separate penalty parameter to be used for each mode. The penalty term is dynamically adjusted until a user defined ratio is achieved.

1.4 Proposed Research

As is evidenced from the literature much work has been done to analyse waveguide structures. The primary goal in all of this work is to identify the first few true modes of the device under study. Hampering the analyses are the so called *spurious* modes, which pollute the solution space and impersonate true modes. Because there is no way to actually determine if the modes being produced are real or not, the waveguide designer must rely on years of practical experience in making an educated guess at the real modes.

The spurious modes are a result of the numerical method used and this is evidenced by the more or less successful methods used in the past. Of these methods, few are general enough to implement in a computer aided design environment. In fact, most of the methods were developed as a result of studying one particular waveguide configuration. This thesis aims to not only implement a finite element based program for solving closed waveguide

problems, but also to propose a method for eliminating spurious modes. The method is based on traditional functionals encountered in previous work but offers a new approach in that the problems are solved using generalized basis vectors that are solenoidal in nature. What is particularly interesting is that the solenoidal basis vectors are computed using the same functional required to find the solutions of the waveguide.

The major thrust of this work will be the use of, and computation of zero-divergence basis vectors. This thesis is divided into 5 chapters. Chapter 1 provides the historical setting for this work. Chapter 2 derives the functional to be used from basis electromagnetic principles. In chapter 3, the derived functional is then transformed into a third order finite element implementation. Chapter 4 presents three case studies of waveguides analysed with this method. Chapter 5 summarizes the major findings and identifies further areas of study.

Chapter 2

The Variational Formulation

Finding the modes of dielectric loaded waveguides is in general not the type of problem that has a closed form, analytic solution. As such, problems of this type must be solved using numerical techniques best suited for computers. With this in mind this chapter will present a variational formulation used to find the modes of dielectric loaded waveguides *without* spurious modes.

The approach is to present Maxwell's equations and continuity conditions and from these derive the fundamental curl-curl equation, also known as the homogeneous vector Helmholtz equation. From this, a variational formulation will be presented which is traditionally used in finding the modes of waveguides. This method, as will be shown, is flawed and so an augmented expression will be derived to be used in conjunction with the traditional approach. Together, these two expressions will form the basis of a variational

method to be later converted into a finite element scheme.

2.1 Introduction

Maxwell's equations form the foundation of electromagnetic theory. As such it would be both reassuring and informative to show that the variational expressions to be used in the analysis of waveguides can be derived explicitly from these fundamental relations. As depicted in figure 2.1, the geometry of the class of waveguides to be analyzed consists of an arbitrarily shaped region uniform in the z-direction clad with a good conductor on all sides. The region Ω, inside the waveguide, may consist of an arbitrary number of materials. Further, it is assumed that there are no sources in the region. Given these assumptions we may derive the classical curl-curl equation.

2.2 The Basic Equations

The time-harmonic Maxwell's equations written in terms of vector field phasors in a simple, source free region may be written as:

$$\nabla \times \mathbf{E} = -j\omega\mu\mathbf{H}, \tag{2.1}$$

$$\nabla \times \mathbf{H} = j\omega\epsilon\mathbf{E}, \tag{2.2}$$

$$\nabla \cdot \epsilon\mathbf{E} = 0, \tag{2.3}$$

$$\nabla \cdot \mu\mathbf{H} = 0. \tag{2.4}$$

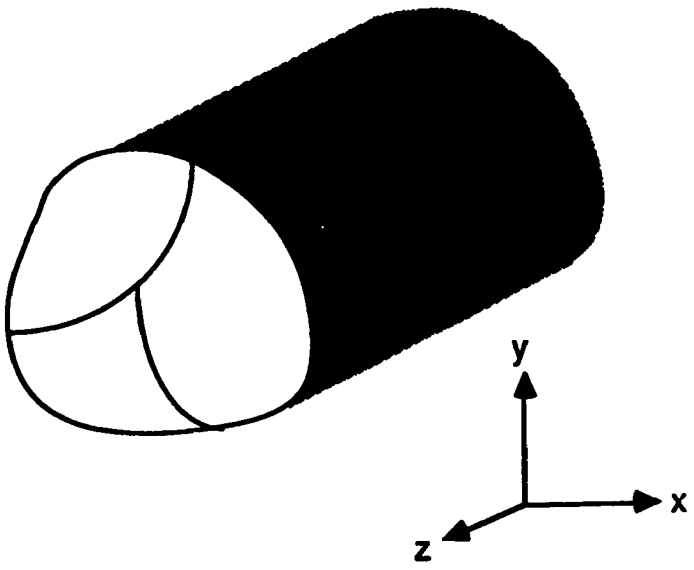

Figure 2.1: General class of waveguides under consideration

This figure depicts the class of waveguides to be considered. The waveguide is assumed to be uniform in the z-direction and completely clad with a good conductor.

Added to this are the constitutive relations:

$$\mathbf{D} = \varepsilon\mathbf{E}, \tag{2.5}$$

$$\mathbf{B} = \mu\mathbf{H}. \tag{2.6}$$

Further, the simple source free region is assumed to have materials with the following properties:

- The materials are linear. That is, they do not depend on **H** or **E**.
- The materials are time invariant. That is, neither ε nor μ vary over time.
- The materials are lossless. That is, ε and μ are both Hermitian.
- The materials are isotropic. That is, ε and μ are scalars.

The boundary rules consistent with Maxwell's equations in integral form can be shown to be equivalent to the following statements:

- On a perfectly conducting boundary $\partial\Omega_S$, the electric field is normal to the surface. This is generally referred to as a *short circuit*. Algebraically, this is represented by any one of the following statements:

$$\mathbf{E}_{\text{tangential}} = 0, \tag{2.7}$$

$$\mathbf{E} \times \mathbf{n} = 0, \tag{2.8}$$

$$(\nabla \times \mathbf{H}) \times \mathbf{n} = 0. \tag{2.9}$$

- On an open boundary $\partial\Omega_O$, the magnetic field is normal to the surface. This is generally referred to as an *open circuit*. Algebraicaly, this is represented by any one of the following statements.

$$\mathbf{H}_{\text{tangential}} = 0, \tag{2.10}$$

$$\mathbf{H} \times \mathbf{n} = 0, \tag{2.11}$$

$$(\nabla \times \mathbf{E}) \times \mathbf{n} = 0. \tag{2.12}$$

With these fundamental equations, we can perform some algebraic manipulations to produce a single second order differential equation along with two boundary conditions.

2.3 The Curl-Curl Equation

We can eliminate either **E** or **H** from equations (2.1) and (2.2) to yield a second order partial differential equation in either **E** or **H** . The latter will be chosen.

Rewriting equation (2.2),

$$j\omega\varepsilon\mathbf{E} = \nabla \times \mathbf{H}, \tag{2.13}$$

and dividing through by $(j\omega\varepsilon)$ we get:

$$\mathbf{E} = \frac{1}{j\omega\varepsilon}\nabla \times \mathbf{H}. \tag{2.14}$$

Taking the curl of both sides of equation (2.14):

$$\nabla \times \mathbf{E} = \nabla \times (\frac{1}{j\omega\varepsilon} \nabla \times \mathbf{H}), \tag{2.15}$$

and substituting using equation (2.1) produces:

$$\nabla \times (\frac{1}{j\omega\varepsilon} \nabla \times \mathbf{H}) = -j\omega\mu\mathbf{H}. \tag{2.16}$$

Multiplying both sides of equation (2.16) by $(j\omega)$ produces the curl-curl equation:

$$\nabla \times (\frac{1}{\varepsilon_r \varepsilon_o} \nabla \times \mathbf{H}) - \omega^2 \mu_r \mu_o \mathbf{H} = 0. \tag{2.17}$$

Equation (2.17) can be further simplified, if we let

$$k^2 = \omega^2 / c^2, \tag{2.18}$$

where c is the speed of light *in vacuo* $= 1/\sqrt{\mu_o \varepsilon_o}$ and we define

$$\mu_r = \mu/\mu_o, \tag{2.19}$$

$$\varepsilon_r = \varepsilon/\varepsilon_o. \tag{2.20}$$

Then we get

$$\nabla \times (1/\varepsilon_r \nabla \times \mathbf{H}) - k^2 \mu_r \mathbf{H} = 0, \tag{2.21}$$

as the revised curl-curl equation. For $k \neq 0$, equation (2.4, implies that

$$\nabla \cdot (1/k^2 \nabla \times (1/\varepsilon_r \nabla \times \mathbf{H})) = 0. \tag{2.22}$$

Thus, for the region Ω, the complete partial differential formulation in just $\mathbf{H}$ is:

$$\nabla \times (1/\varepsilon_r \nabla \times \mathbf{H}) - k^2 \mu_r \mathbf{H} = 0 \tag{2.23}$$

with boundary conditions:

$$(\nabla \times \mathbf{H}) \times \mathbf{n} = 0 \quad \text{on } \partial\Omega_S \tag{2.24}$$

$$\mathbf{H} \times \mathbf{n} = 0 \quad \text{on } \partial\Omega_O \tag{2.25}$$

We have thus derived the so-called homogeneous vector Helmholtz equation in terms of a phasor vector field **H**. We are left to find a functional that has this vector Helmholtz equation as its corresponding Euler equation.

2.4 The Functional

Assuming for the sake of simplicity that $\mu_r = 1$, a variational formulation equivalent to equations (2.23) through (2.25) would be: Find pairs $(\mathbf{H}, k)$ such that the functional

$$F(\mathbf{H}) = \frac{1}{2}\int_\Omega [|\nabla \times \mathbf{H}|^2/\epsilon_r - k^2|\mathbf{H}|^2]d\Omega. \tag{2.26}$$

is at a stationary point, subject to:

$$(\mathbf{H} \times \mathbf{n}) = 0 \quad \text{on } \partial\Omega_O. \tag{2.27}$$

Unfortunately, the boundary value problem in **H** and the corresponding variational formulation lead to a numerical method which is flawed. Both the boundary value problem and the variational formulation have infinitely many solutions with zero frequency.

2.4.1 Spurious modes

Consider for example the class of solutions satisfying the following:

$$\mathbf{H} = \nabla\phi, \tag{2.28}$$

$$k = 0. \tag{2.29}$$

From equation (2.21) and the vector identity

$$\nabla \times \nabla\phi = 0, \tag{2.30}$$

any ϕ will satisfy the functional for $k = 0$. In numerical schemes, the trial functions tend to approximate these zero-frequency solutions and hence we get spurious modes. We can reduce the infinite number of zero-frequency modes to a finite number by imposing two extra constraints:

$$\nabla \cdot \mathbf{H} = 0 \quad \text{in } \Omega \text{ and,} \tag{2.31}$$

$$\mathbf{H} \cdot \mathbf{n} = 0 \quad \text{on } \partial\Omega_S. \tag{2.32}$$

Notice that neither of these constraints changes the solutions for $k > 0$ since each constraint is implied by the original equations. We have already seen from equation (2.23) that

$$\nabla \times (1/\varepsilon_r \nabla \times \mathbf{H}) - k^2\mathbf{H} = 0. \tag{2.33}$$

After some algebraic manipulations, equation (2.33) can be rewritten as:

$$\mathbf{H} \cdot \mathbf{n} = 1/(k^2)\nabla \times (1/\varepsilon_r \nabla \times \mathbf{H}) \cdot \mathbf{n}. \tag{2.34}$$

So from equation (2.9),

$$(1/\varepsilon_r \nabla \times \mathbf{H}) \times \mathbf{n} = 0 \qquad \text{on } \partial\Omega_S \tag{2.35}$$

implies that,

$$\nabla \times (1/\varepsilon_r \nabla \times \mathbf{H}) \cdot \mathbf{n} = 0 \qquad \text{on } \partial\Omega_S. \tag{2.36}$$

From (2.34) and (2.36):

$$\mathbf{H} \cdot \mathbf{n} = 0 \qquad \text{on } \partial\Omega_S. \tag{2.37}$$

For $k = 0$ we get:

$$\nabla \times (1/\varepsilon_r \nabla \times \mathbf{H}) = 0 \qquad \text{in } \Omega, \tag{2.38}$$

and,

$$\mathbf{H} \cdot \mathbf{n} = 0 \qquad \text{on } \partial\Omega_S \tag{2.39}$$

implies that

$$(\nabla \times \mathbf{H}) \times \mathbf{n} = 0. \tag{2.40}$$

This can be shown to have at most a finite number of solutions. Summarizing, the revised boundary value problem is:

$$\nabla \times (1/\varepsilon_r \nabla \times \mathbf{H}) - k^2 \mathbf{H} = 0 \qquad \text{in } \Omega \tag{2.41}$$

$$\nabla \cdot \mathbf{H} = 0 \qquad \text{in } \Omega \tag{2.42}$$

$$\mathbf{H} \cdot \mathbf{n} = 0 \qquad \text{on } \partial\Omega_S \tag{2.43}$$

$$(\nabla \times \mathbf{H}) \times \mathbf{n} = 0 \qquad \text{on } \partial\Omega_S \tag{2.44}$$

$$\mathbf{H} \times \mathbf{n} = 0 \qquad \text{on } \partial\Omega_O \tag{2.45}$$

Variational formulations used by others have tried to ensure that

$$\nabla \cdot \mathbf{H} = 0 \qquad \text{in } \Omega \text{ and} \tag{2.46}$$

$$\mathbf{H} \cdot \mathbf{n} = 0 \qquad \text{on } \partial\Omega_S. \tag{2.47}$$

Of the more popular methods in use, the appropriately named *Penalty Method* penalizes divergent solutions by adding a term to the traditional functional. Because of its significance to this work, the method will be described here.

2.4.2 The Penalty Method

The penalty method adds a new term to the traditional functional defined in equation (2.26). The modified functional with the added term is:

$$F_p(\mathbf{H}) = \frac{1}{2}\int_\Omega [|\nabla \times \mathbf{H}|^2/\epsilon_r + s|\nabla \cdot \mathbf{H}|^2 - k^2|\mathbf{H}|^2]d\Omega, \tag{2.48}$$

where the new term

$$s|\nabla \cdot \mathbf{H}|^2 \tag{2.49}$$

has been added to the functional. The purpose of the s parameter is to weight a term that in effect penalizes **H** solutions with non-zero divergence. By increasing the s parameter, the eigenvalues of solutions affected by the divergence term are pushed out of the spectrum of interest.

Problems still arise with this method since we do not know in advance how big s should be. Care must also be taken not to make s too large, however, as

we would no longer be solving the original functional since the curl expression would become negligible. In practice, the penalty method works reasonably well for inherently two dimensional problems since increasing the s parameter causes eigenvalues of the spurious modes to *shift right* when plotted on a number line. This *right shift* phenomena gives the illusion that spurious modes are being eliminated, but in reality they are simply pushed out of the spectrum of interest.

Repeated solutions varying s reveals that the true modes tend to remain stationary whereas spurious modes vary in position according to s. Herein lies the *modus operandi* of the Penalty Method.

2.5 The Augmented Functional

An alternative to penalyzing the solution space is to ensure that the trial functions themselves obey the zero-divergence condition and the associated boundary conditions *a priori*.

Let P represent a space of vector trial functions over Ω. Let S be the space of solenoidal elements of P. By finding a suitable basis for S, we are assured that all solutions consisting of linear combinations of these basis vectors lie within the space of solenoidal solutions and so satisfy the zero divergence condition.

It is easy to see how previous work led to shrinking the solution space in

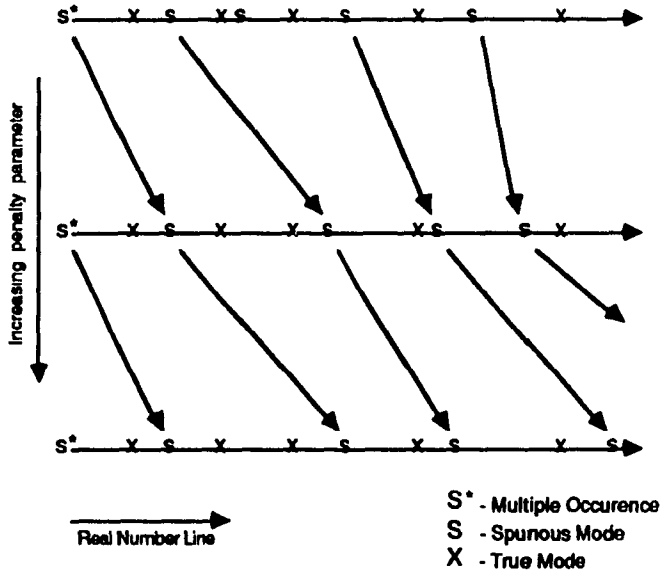

Figure 2.2: Migrating modes

This figure depicts what happens when the s parameter is increased. The eigenvalues of the spurious modes migrate to the right. The true modes are slightly perturbed due to the contribution of the s term. By repeatedly solving the problem for varying s, spurious modes become self evident.

some manner by imposing more constraints on the basis vectors. To date no method has removed all the spurious modes in a general way but all methods have more or less succeeded in making the system less flexible.

Thus the task is now to find a set of basis vectors that span the solonoidal space of solutions and no more. This is similar to requesting that all linearly independent solonoidal vectors spanning the region be found. It is clear that this in itself is a valid boundary value problem and that a variational formulation is entirely suited for this.

Previously, we stated that the functional in equation (2.26) alone gave problems. A modified version of that functional which penalized divergent solutions showed promise but failed in that the spurious modes were still there but simply pushed out of the spectrum of interest. We wish to find divergence free basis vectors in the region of interest. There are several approaches to solving this problem. One method would be to explicitly define solonoidal functions over each element, much like Nassif [37] did in her doctoral dissertation. The drawback of Nassif's functions were that they did not enforce normal continuity of the field at inter-element boundaries.

Another approach would be to compute anew the trial functions numerically, for each geometry, and to essentially dispense with computing localized solenoidal basis vectors over each element. This approach has an inherent simplicity since inter-element continuity is ensured at the expense of generating globally defined basis vectors.

We propose the following alternate functional:

$$K_{ab}(\mathbf{H}) = \frac{1}{2}\int_{\Omega}[a|\nabla \times \mathbf{H}|^2/\epsilon_r + b|\nabla \cdot \mathbf{H}|^2 - k^2|\mathbf{H}|^2]d\Omega. \qquad (2.50)$$

where $a, b \in (0,1)$ and $a \neq b$. Notice the similarity between this functional and the two previous functionals, defined in (2.26) and (2.48). We claim that from this functional alone, we can not only find the solutions of the waveguide problem but also generate the set of linearly independent solonoidal trial functions. By solving the functional with $a = 0$ and $b = 1$ (K_{01}), subject to the initial boundary conditions imposed by Maxwell's equations and the geometry of the problem, we arrive at a series of eigensolutions corresponding to $k = 0$. The number of eigensolutions produced is finite and correspond identically to zeroes of the functional. Mathematically, the divergence of the eigenvectors corresponding to each of the 0-eigenvalues is zero and so form a basis for the set of solonoidal basis vectors spanning the region. Not only do the basis vectors span the region, they also satisfy the initial boundary conditions.

If the eigenvectors corresponding to 0-eigenvalues are stored for later use, it is easy to see how the eigenvectors themselves may be reused as trial functions in the solution of the K_{10} functional. Solving the K_{10} functional without imposing boundary conditions, since the boundary conditions are satisfied by the original basis vectors, will yield a set of non-zero eigensolutions corresponding to the true modes of the waveguide.

Summarizing, the K-Functional along with the standard boundary conditions fornd above together form the foundation for a variational formulation

that will not only yield the true modes of a dielectric loaded waveguide but also generate the trial functions used in computing those modes.

2.6 Summary

In this chapter, we derived a modified functional that will be used in subsequent chapters as the foundation of a numerical method aimed at eliminating spurious modes encountered in waveguide analysis.

The approach was to derive the curl-curl equation directly from Maxwell's equations and from there propose a variational formulation which has as it's Euler equation, the curl-curl equation.

We saw that such functionals alone caused problems in the past. Many solutions to these problems were presented in Chapter 1 and we saw that the one major characteristic of spurious modes was their non-zero divergence.

A method was proposed to define trial functions that would have zero-divergence throughout the region and at the same time obey the initial boundary conditions. These trial functions would then be used to solve the standard functional and thus eliminate any spurious modes.

In the next chapter, the finite element implementation of this new functional will be presented.

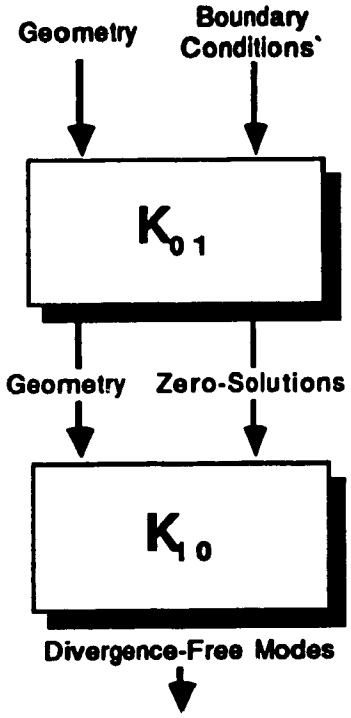

Figure 2.3: Two step approach to finding the solutions of the waveguide problem.

This figure depicts the two step approach to finding the solutions of the waveguide problem. The first step is to solve the K_{01} functional, using as input the original boundary conditions of the problem as well as the geometry. Solutions corresponding to 0-eigenvalues are identically solonoidal and so form a basis spanning the region. The eigenvectors are stored to be used in the second step where the K_{10} functional is solved. The solutions of this second step are identically solonoidal and hence correspond to real solutions of the waveguide problem.

Chapter 3

The Finite Element Implementation

In the previous chapter we derived directly from Maxwell's equations a functional, along with suitable boundary conditions, that would not only yield divergence free basis vectors that spanned the solution space of the problem but also provide the true modes of the waveguide. For the functional to be of any use in a computer aided environment, it must be transformed into a numerical scheme.

In this chapter, a matrix representation will be derived that will allow us to implement the functional in a finite element program.

3.1 Matrix representation of the functional

It was shown previously that the stationary points of the functional

$$K_{ab}(\mathbf{H}) = \int_{\Omega} [a|\nabla \times \mathbf{H}|^2/\epsilon_r + b|\nabla \cdot \mathbf{H}|^2 - k^2|\mathbf{H}|^2] d\Omega, \tag{3.1}$$

subject to certain essential boundary conditions, is enough to define divergence free basis vectors and produce the correct modes of the waveguide.

It will be shown that the functional in equation (3.1) may be transformed using standard finite element techniques into:

$$K_{ab}(\mathbf{x}) = \mathbf{x}^t(a\mathbf{A} + b\mathbf{C} - k^2\mathbf{B})\mathbf{x} \tag{3.2}$$

where $a, b \in \{0, 1\}$ and $a \neq b$; $\mathbf{A}$, $\mathbf{B}$, and $\mathbf{C}$ are $n \times n$ real symmetric matrices; $\mathbf{x}$ is a real vector of the n-remaining degrees of freedom in the discretized problem after boundary conditions are imposed. Equating (3.1) and (3.2):

$$\int_{\Omega} |\nabla \times \mathbf{H}|^2/\epsilon_r = \mathbf{x}^t\mathbf{A}\mathbf{x}, \tag{3.3}$$

$$\int_{\Omega} |\mathbf{H}|^2 d\Omega = \mathbf{x}^t\mathbf{B}\mathbf{x}, \tag{3.4}$$

$$\int_{\Omega} |\nabla \cdot \mathbf{H}|^2 = \mathbf{x}^t\mathbf{C}\mathbf{x}. \tag{3.5}$$

The stationary points of equation (3.2) are found by taking the first variation with respect to $\mathbf{x}$ and solving

$$a\mathbf{A}\mathbf{x} + b\mathbf{C}\mathbf{x} - k^2\mathbf{B}\mathbf{x} = \mathbf{0}. \tag{3.6}$$

Because of the conditions on a, and b, this leads to two algebraic eigenvalue problems:

$$\mathbf{Ax} = k^2\mathbf{Bx}, \tag{3.7}$$

and

$$\mathbf{Cx} = k^2\mathbf{Bx}. \tag{3.8}$$

It is apparent that finding the stationary points of our functional reduces to finding explicit representations for the three matrices, **A**, **B**, and **C**. Once these expressions are found, the matrices may be constructed and the system of equations solved using a general eigenvalue solver.

3.1.1 Simplifying the expressions

The functional is decomposed into three term:

$$K_{ab}(\mathbf{H}) = aK_1(\mathbf{H}) + bK_2(\mathbf{H}) - k^2K_3(\mathbf{H}), \tag{3.9}$$

where

$$K_1(\mathbf{H}) = \mathbf{x}^t\mathbf{Ax}, \tag{3.10}$$

$$K_2(\mathbf{H}) = \mathbf{x}^t\mathbf{Cx}, \tag{3.11}$$

$$K_3(\mathbf{H}) = \mathbf{x}^t\mathbf{Bx}. \tag{3.12}$$

We can express **H** as a linear combination of global basis vectors, Φ:

$$\mathbf{H} = \sum_{i=1}^{n} \Phi_i x_i, \tag{3.13}$$

where

$$\Phi_i = (\phi_{ix}, \phi_{iy}, j\phi_{iz}), \tag{3.14}$$

and n represents the total number of trial functions to be used. $\phi_{ix}, \phi_{iy}, \phi_{iz}$ are real, because the problem is lossless.

3.1.2 Solving for K_1

By substituting equation (3.13) into equation (3.3) we get:

$$K_1(\mathbf{H}) = \int_\Omega [\frac{1}{\epsilon_r}(\nabla \times \sum_{i=1}^{n} \Phi_i x_i)^* \cdot (\nabla \times \sum_{j=1}^{n} \Phi_j x_j)] d\Omega. \tag{3.15}$$

It can be shown that

$$\nabla \times \sum_{i=1}^{n} \Phi_i x_i = \sum_{i=1}^{n} x_i \nabla \times \Phi_i. \tag{3.16}$$

Using the above relation, equation (3.15) becomes

$$K_1(\mathbf{H}) = \int_\Omega [\sum_{i=1}^{n}\sum_{j=1}^{n} x_i x_j \frac{1}{\epsilon_r}(\nabla \times \Phi_i)^* \cdot (\nabla \times \Phi_j)] d\Omega, \tag{3.17}$$

or

$$K_1(\mathbf{H}) = \sum_{i=1}^{n}\sum_{j=1}^{n} x_i x_j \frac{1}{\epsilon_r} \int_\Omega [(\nabla \times \Phi_i)^* \cdot (\nabla \times \Phi_j)] d\Omega \tag{3.18}$$

where terms unaffected by the integration are moved outside the integral. Notice that here we make the assumption that ϵ_r is constant over each element. From this, A_{ij} may be expressed as:

$$A_{ij} = \frac{1}{\epsilon_r} \int_\Omega [(\nabla \times \Phi_i)^* \cdot (\nabla \times \Phi_j)] d\Omega, \tag{3.19}$$

and hence, the complete expression for K_1 is

$$K_1(\mathbf{H}) = \sum_{i=1}^{n}\sum_{j=1}^{n} x_i A_{ij} x_j. \tag{3.20}$$

3.1.3 Solving for K_3

By substituting equation (3.13) into equation (3.4) we get:

$$K_3(\mathbf{H}) = \int_{\Omega} [(\sum_{i=1}^{n} \Phi_i x_i)^* \cdot (\sum_{j=1}^{n} \Phi_j x_j)] d\Omega. \tag{3.21}$$

Grouping similar terms and rearranging the terms under the intergal we get:

$$K_3(\mathbf{H}) = \int_{\Omega} \sum_{i=1}^{n}\sum_{j=1}^{n} x_{i_{\alpha_j}} \Phi_i^* \cdot \Phi_j) d\Omega, \tag{3.22}$$

or

$$K_3(\mathbf{H}) = \sum_{i=1}^{n}\sum_{j=1}^{n} x_i x_j \int_{\Omega} (\Phi_i^* \cdot \Phi_j) d\Omega, \tag{3.23}$$

where terms not affected by the integration are removed from beneath the intergal. From this, B_{ij} may be expressed as:

$$B_{ij} = \int_{\Omega} (\Phi_i^* \cdot \Phi_j) d\Omega, \tag{3.24}$$

and hence, the complete expression for K_3 is

$$K_3(\mathbf{H}) = \sum_{i=1}^{n}\sum_{j=1}^{n} x_i B_{ij} x_j. \tag{3.25}$$

3.1.4 Solving for K_2

By substituting equation (3.13) into equation (3.5) we get:

$$K_2(\mathbf{H}) = \int_{\Omega} (\nabla \cdot \sum_{i=1}^{n} \Phi_i x_i)^* (\nabla \cdot \sum_{j=1}^{n} \Phi_j x_j) d\Omega, \tag{3.26}$$

or after suitable manipulation,

$$K_2(\mathbf{H}) = \sum_{i=1}^{n} \sum_{j=1}^{n} x_i x_j \int_{\Omega} (\nabla \cdot \Phi_i)^* (\nabla \cdot \Phi_j) d\Omega. \tag{3.27}$$

An expression for C_{ij} is thus:

$$C_{ij} = \int_{\Omega} (\nabla \cdot \Phi_i)^* (\nabla \cdot \Phi_j) d\Omega, \tag{3.28}$$

or in terms of K_2

$$K_2(\mathbf{H}) = \sum_{i=1}^{n} \sum_{j=1}^{n} x_i C_{ij} x_j. \tag{3.29}$$

3.2 Third-order FEM expressions for A_{ij}, B_{ij} and C_{ij}

The global basis vectors Φ_i are represented on each triangle by Lagrange interpolation polynomials:

$$\Phi_i = (\sum_{l=1}^{10} u_{xil} \alpha_l, \sum_{l=1}^{10} u_{yil} \alpha_l, \sum_{l=1}^{10} j u_{zil} \alpha_l) \tag{3.30}$$

where the u_{xil}'s are assumed to be values of Φ_i at the ten nodes of the triangle and the α_l's are interpolation polynomials of the form

$$\alpha_l = R_i(\nu, \zeta_1) R_j(\nu, \zeta_2) R_k(\nu, \zeta_3) \tag{3.31}$$

where

$$R_m(\nu, \zeta) = \prod_{k=0}^{m-1} \frac{\zeta - k/\nu}{m/\nu - k/\nu} \tag{3.32}$$

$$= \frac{1}{m!} \prod_{k=0}^{m-1} (\nu\zeta - k) \tag{3.33}$$

for $m > 0$, and

$$R_0(\nu, \zeta) = 1. \tag{3.34}$$

The variable ν represents the element order[1]. The single subscript l represents the triple indexed alpha polynomial[2] corresponding to node l on the third order element.

Computing the third order finite element matrix representation amounts to defining three general expressions found in equations (3.19), (3.24) and (3.28).

[1]Order 3 was chosen in the present work to provide for sufficient accuracy with a small number of elements.

[2]See [19].

3.2.1 Computing the A matrix

From equation (3.19) we see that the general expression

$$(\nabla \times \Phi_i) \tag{3.35}$$

is required to compute the **A** matrix.

The operator ∇ is defined to be the standard rectangular coordinate system, *del* operator. However in the context of phasor analysis we can show that derivatives with respect to the time variable t, correspond to $j\omega$, and to the z-axis, $-j\beta$. Thus without loss of generality, we may define:

$$\nabla \equiv (\frac{\partial}{\partial x}, \frac{\partial}{\partial y}, -j\beta). \tag{3.36}$$

Using equation (3.36), the complete expression for equation (3.35) becomes:

$$(\nabla \times \Phi_i) = j(\frac{\partial \phi_{iz}}{\partial y} + \beta\phi_{iy}, \frac{-\partial \phi_{iz}}{\partial x} - \beta\phi_{ix}, \frac{\partial \phi_{iy}}{\partial x} - \frac{\partial \phi_{ix}}{\partial y}) \tag{3.37}$$

From equation (3.30) the general expression for a single component of Φ_i is:

$$\phi_{is} = \sum_{l=1}^{10} u_{sil}\alpha_l \tag{3.38}$$

where $s \in \{x, y, z\}$. Thus computing the partial derivatives with respect to a generic variable v, we get:

$$\frac{\partial \phi_{is}}{\partial v} = \frac{\partial}{\partial v}(\sum_{l=1}^{10} u_{sil}\alpha_l) \tag{3.39}$$

$$= \sum_{l=1}^{10} u_{sil} \frac{\partial \alpha_l}{\partial v} \tag{3.40}$$

$$= \sum_{l=1}^{10} u_{sil} \sum_{p=1}^{3} \frac{\partial \alpha_l}{\partial \zeta_p} \frac{\partial \zeta_p}{\partial v} \tag{3.41}$$

$$= \sum_{l=1}^{10} u_{sil} M_{lv} \tag{3.42}$$

Substituting equation (3.42) into equation (3.37) yields:

$$\begin{aligned} (\nabla \times \Phi_i) \;=\; & j\Big(\sum_{l=1}^{10} u_{xil} M_{ly} + \beta \sum_{l=1}^{10} u_{yi} \alpha_l, \\ & -\sum_{l=1}^{10} u_{zil} M_{lx} - \beta \sum_{l=1}^{10} u_{xi} \alpha_l, \\ & \sum_{l=1}^{10} u_{yil} M_{lx} - \sum_{l=1}^{10} u_{xi} M_{ly}\Big) \end{aligned} \tag{3.43}$$

A more convenient notation for equation (3.43) allows us to express the curl operator as three dot products of a common vector u. Let

$$(\nabla \times \Phi_i) = j(\mathbf{m}_x^t \cdot \mathbf{u}_i, \mathbf{m}_y^t \cdot \mathbf{u}_i, \mathbf{m}_z^t \cdot \mathbf{u}_i), \tag{3.44}$$

where $\mathbf{u}_i$ is defined as:

$$\mathbf{u}_i^t \equiv [u_{xi1} u_{xi2} \ldots u_{xi10} | u_{yi1} u_{yi2} \ldots u_{yi10} | u_{zi1} u_{zi2} \ldots u_{zi10}] \tag{3.45}$$

corresponding to the ten xyz components of the locally defined global basis vector, Φ_i.

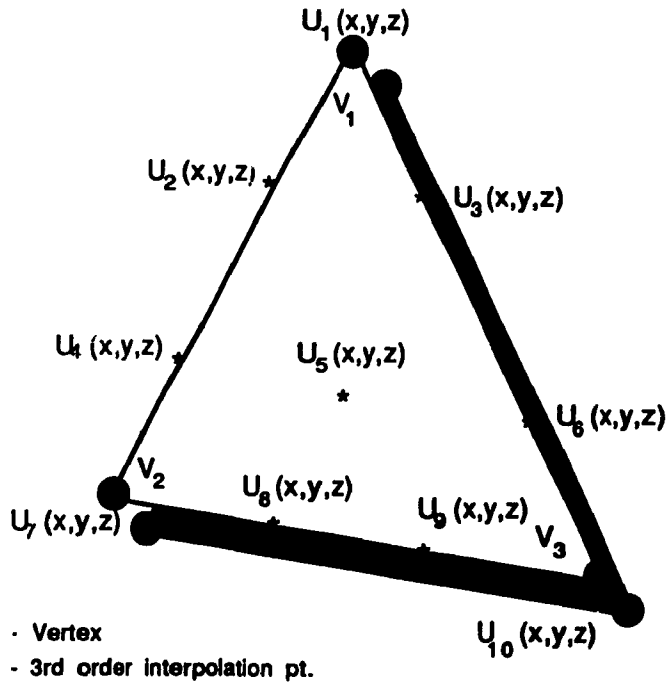

Figure 3.1: Mapping of the u vector onto a 3rd order element.

This figure depicts the relationship between a newly defined local* u *vector and the coordinates of a higher order element. As will be seen later, this newly defined vector simplifies the local assembly process associated with the finite element method. In turn, the globally defined basis vectors may then be mapped onto each element by making use of the* u *vector.

It follows from this definition of u that:

$$\mathbf{m}_x^t = [0,0,\ldots,0|\beta\alpha_1,\beta\alpha_2,\ldots,\beta\alpha_{10}|M_{1y},M_{2y},\ldots,M_{10y}] \quad (3.46)$$

$$\mathbf{m}_y^t = [-\beta\alpha_1,-\beta\alpha_2,\ldots,-\beta\alpha_{10}|0,0,\ldots,0| -M_{1x},-M_{2x},\ldots,-M_{10x}] \quad (3.47)$$

$$\mathbf{m}_z^t = [-M_{1y},-M_{2y},\ldots,-M_{10y}|M_{1x},M_{2x},\ldots,M_{10x}|0,0,\ldots,0] \quad (3.48)$$

Taking the dot product of the curl expressions we get:

$$\begin{aligned}(\nabla\times\Phi_i)^*\cdot(\nabla\times\Phi_j) &= (\mathbf{u}_i^t\cdot\mathbf{m}_x)(\mathbf{m}_x^t\cdot\mathbf{u}_j)\\ &\quad +(\mathbf{u}_i^t\cdot\mathbf{m}_y)(\mathbf{m}_y^t\cdot\mathbf{u}_j)\\ &\quad +(\mathbf{u}_i^t\cdot\mathbf{m}_z)(\mathbf{m}_z^t\cdot\mathbf{u}_j)\\ &= \mathbf{u}_i^t\cdot\mathbf{M}\cdot\mathbf{u}_j, \end{aligned} \quad (3.49)$$

where

$$\mathbf{M} = \mathbf{m}_x\cdot\mathbf{m}_x{}^t + \mathbf{m}_y\cdot\mathbf{m}_y{}^t + \mathbf{m}_z\cdot\mathbf{m}_z{}^t. \quad (3.50)$$

Thus a single component of **A** defined in terms of a third order finite element implementation becomes:

$$A_{ij} = \frac{1}{\epsilon_r}\mathbf{u}_i^t\cdot\int_\Omega \mathbf{M}d\Omega\cdot\mathbf{u}_j. \quad (3.51)$$

3.2.2 Computing the B matrix

From equation (3.24) the general expression

$$(\Phi_i^*\cdot\Phi_j) \quad (3.52)$$

is required to compute the **B** matrix. Defining Φ_i as three dot products of a common vector u:

$$\Phi_i = (\mathbf{n}_x^t \cdot \mathbf{u}_i, \mathbf{n}_y^t \cdot \mathbf{u}_i, j\mathbf{n}_z^t \cdot \mathbf{u}_i). \tag{3.53}$$

It follows from the definition of u in (3.45) that:

$$\mathbf{n}_x^t = [\alpha_1, \alpha_2, \alpha_3, \ldots, \alpha_{10} | 0, 0, \ldots, 0 | 0, 0, \ldots, 0] \tag{3.54}$$

$$\mathbf{n}_y^t = [0, 0, \ldots, 0 | \alpha_1, \alpha_2, \ldots, \alpha_{10} | 0, 0, \ldots, 0 |] \tag{3.55}$$

$$\mathbf{n}_z^t = [0, 0, \ldots, 0 | 0, 0, \ldots, 0 | \alpha_1, \alpha_2, \ldots, \alpha 10]. \tag{3.56}$$

Taking the dot product:

$$\begin{aligned} (\Phi_i^* \cdot \Phi_j) &= (\mathbf{u}_i^t \cdot \mathbf{n}_x)(\mathbf{n}_x^t \cdot \mathbf{u}_i) + \\ &\quad (\mathbf{u}_i^t \cdot \mathbf{n}_y)(\mathbf{n}_y^t \cdot \mathbf{u}_i) + \\ &\quad (\mathbf{u}_i^t \cdot \mathbf{n}_z)(\mathbf{n}_z^t \cdot \mathbf{u}_i), \\ &= \mathbf{u}_i^t \cdot \mathbf{N} \cdot \mathbf{u}_j, \end{aligned} \tag{3.57}$$

where

$$\mathbf{N} = \mathbf{n}_x \cdot \mathbf{n}_x{}^t + \mathbf{n}_y \cdot \mathbf{n}_y{}^t + \mathbf{n}_z \cdot \mathbf{n}_z{}^t. \tag{3.58}$$

Thus a single component of **B** defined in terms of a third order finite element implementation becomes:

$$B_{ij} = \mathbf{u}_i^t \cdot \int_\Omega \mathbf{N} d\Omega \cdot \mathbf{u}_j. \tag{3.59}$$

3.2.3 Computing the C matrix

From equation (3.28), the general expression

$$(\nabla \cdot \Phi_i) \tag{3.60}$$

is required to compute the C matrix. Defining $(\nabla \cdot \Phi_i)$ as three dot products of a common vector u:

$$(\nabla \cdot \Phi_i) = \mathbf{p}_x^t \cdot \mathbf{u}_i + \mathbf{p}_y^t \cdot \mathbf{u}_i + \mathbf{p}_z^t \cdot \mathbf{u}_i, \tag{3.61}$$

It follows from the definition of u in (3.45) that:

$$\mathbf{p}_x^t = [M_{1x}, M_{2x}, \ldots, M_{10x} | 0, 0, \ldots, 0 | 0, 0, \ldots, 0] \tag{3.62}$$

$$\mathbf{p}_y^t = [0, 0, \ldots, 0 | M_{1y}, M_{2y}, \ldots, M_{10y} | 0, 0, \ldots, 0] \tag{3.63}$$

$$\mathbf{p}_z^t = [0, 0, \ldots, 0 | 0, 0, \ldots, 0 | -\beta\alpha_1, -\beta\alpha_2, \ldots, -\beta\alpha_{10}]. \tag{3.64}$$

Taking the dot product:

$$\begin{aligned} (\nabla \cdot \Phi_i)^*(\nabla \cdot \Phi_j) &= (\mathbf{u}_i^t \cdot \mathbf{p}_x)(\mathbf{p}_x^t \cdot \mathbf{u}_j) \\ &\quad +(\mathbf{u}_i^t \cdot \mathbf{p}_y)(\mathbf{p}_y^t \cdot \mathbf{u}_j) \\ &\quad +(\mathbf{u}_i^t \cdot \mathbf{p}_z)(\mathbf{p}_z^t \cdot \mathbf{u}_j) \\ &= \mathbf{u}_i^t \cdot \mathbf{P} \cdot \mathbf{u}_j, \end{aligned} \tag{3.65}$$

where

$$\mathbf{P} = \mathbf{p}_x \cdot \mathbf{p}_x{}^t + \mathbf{p}_y \cdot \mathbf{p}_y{}^t + \mathbf{p}_z \cdot \mathbf{p}_z{}^t. \tag{3.66}$$

Thus a single component of C defined in terms of a third order finite element implementation becomes:

$$C_{ij} = \mathbf{u}_i^t \cdot \int_\Omega \mathbf{P} d\Omega \cdot \mathbf{u}_j \tag{3.67}$$

3.3 Integrating M, N, and P

The expressions found in equations (3.51), (3.59), and (3.67) are defined in terms of the integral of three subsidiary matrices, **M**, **N**, and **P**. Integrating each of these matrix expressions amounts to integrating each of their components.

3.3.1 The M matrix

From (3.50) and (3.46) through (3.48) the matrix **M** is completely defined by:

$$\mathbf{M} = \begin{pmatrix} \Gamma_{11} & \Gamma_{12} & \Gamma_{13} \\ \Gamma_{21} & \Gamma_{22} & \Gamma_{23} \\ \Gamma_{31} & \Gamma_{32} & \Gamma_{33} \end{pmatrix} \tag{3.68}$$

where:

$$\Gamma_{11} = \beta^2 \alpha_i \alpha_j + M_{iy} M_{jy} \tag{3.69}$$

$$\Gamma_{12} = -M_{iy} M_{jx} \tag{3.70}$$

$$\Gamma_{13} = \beta \alpha_i M_{jx} \tag{3.71}$$

$$\Gamma_{21} = -M_{ix} M_{jy} \tag{3.72}$$

$$\Gamma_{22} = \beta^2 \alpha_i \alpha_j + M_{ix} M_{jx} \tag{3.73}$$

$$\Gamma_{23} = \beta \alpha_i M_{jy} \tag{3.74}$$

$$\Gamma_{31} = \beta \alpha_j M_{ix} \tag{3.75}$$

$$\Gamma_{32} = \beta\alpha_j M_{iy} \tag{3.76}$$

$$\Gamma_{33} = M_{iy}M_{jy} + M_{iz}M_{jz} \tag{3.77}$$

Examining equations (3.69) through (3.77) reveals three common expressions:

$$\beta^2\alpha_i\alpha_j \tag{3.78}$$

$$\beta\alpha_i M_{jz} \tag{3.79}$$

$$M_{iz}M_{jt} \tag{3.80}$$

Computing the integral of (3.68) necessitates computing the integral of the terms found in (3.78) through (3.80).

Computing the integral of (3.78):

$$\beta^2 \int_{\Omega} \alpha_i\alpha_j d\Omega = \triangle\beta^2 T_{ij}^{(3)}, \tag{3.81}$$

where the $T_{ij}^{(3)}$ are known results that have been previously published[3], and $\triangle$ represents the area of the element.

Computing the integral of (3.79) requires the integration of a previously defined quantity, M_{lz}. Since the α polynomials are themselves a function of the ζ's, we may represent the derivative of an n^{th} order α polynomial as a

[3]See for example [4], and [5].

linear combination of n^{th} order α polynomials[4]. That is:

$$\frac{\partial \alpha_l}{\partial \zeta_p} \equiv \sum_{k=1}^{10} D_{lk}{}^{(p)} \alpha_k{}^{(3)}, \tag{3.82}$$

where

$$D_{lk}{}^{(p)} \equiv \frac{\partial \alpha_l^{(3)}}{\partial \zeta_p} \Big|_{P_k{}^{(3)}} \tag{3.83}$$

and $P_k{}^{(3)}$ indicates that the expression is evaluated at each of the k interpolation nodes of a 3rd order element.

Thus with the expression M_{ls} defined as:

$$M_{ls} = \sum_{p=1}^{3} \sum_{k=1}^{10} D_{lk}{}^{(p)} \alpha_k{}^{(p)} \frac{\partial \zeta_p}{\partial s} \tag{3.84}$$

we compute the integral of (3.79):

$$\beta \int_\Omega \alpha_i M_{js} d\Omega = \beta \int_\Omega \alpha_i \sum_{p=1}^{3} \sum_{k=1}^{10} D_{jk}{}^{(p)} \alpha_k{}^{(3)} \frac{\partial \zeta_p}{\partial s} d\Omega \tag{3.85}$$

$$= \beta \sum_{p=1}^{3} \sum_{k=1}^{10} D_{jk}{}^{(p)} \frac{\partial \zeta_p}{\partial s} \int_\Omega \alpha_i \alpha_k{}^{(3)} d\Omega \tag{3.86}$$

$$= \Delta\beta \sum_{p=1}^{3} \sum_{k=1}^{10} D_{jk}{}^{(p)} \frac{\partial \zeta_p}{\partial s} \mathrm{T}_{ik}{}^{(3)}. \tag{3.87}$$

[4]See [19].

With the result generated in equation (3.84), the integral of (3.80) is:

$$\int_{\Omega} M_{is} M_{jt} d\Omega = \int_{\Omega} \sum_{p=1}^{3} \sum_{k=1}^{10} D_{ik}{}^{(p)} \alpha_k{}^{(3)} \frac{\partial \zeta_p}{\partial s} \sum_{q=1}^{3} \sum_{l=1}^{10} D_{jl}{}^{(q)} \alpha_l{}^{(3)} \frac{\partial \zeta_q}{\partial t} d\Omega \quad (3.88)$$

$$= \Delta \sum_{p=1}^{3} \sum_{k=1}^{10} D_{ik}{}^{(p)} \frac{\partial \zeta_p}{\partial s} \sum_{q=1}^{3} \sum_{l=1}^{10} D_{jl}{}^{(q)} \frac{\partial \zeta_q}{\partial t} \mathrm{T}_{kl}{}^{(3)}. \quad (3.89)$$

Clearly computing this quantity each time for each element is very CPU intensive. A more efficient approach would be to precompute as much as possible[5] *a priori*. it is readily apparent from equation (3.87) that the following expression is independent of element shape and orientation, and hence may be calculated once and for all for every i,j, and p. The result is a triply indexed array:

$$U_2(i,j,p) = \sum_{p=1}^{3} \sum_{k=1}^{10} D_{jk}{}^{(p)} \mathrm{T}_{ik}{}^{(3)} \quad (3.90)$$

Similarly, equation (3.89) reveals that

$$U_1(i,j,p,q) = \sum_{p=1}^{3} \sum_{k=1}^{10} D_{ik}{}^{(p)} \sum_{q=1}^{3} \sum_{l=1}^{10} D_{jl}{}^{(q)} \mathrm{T}_{kl}{}^{(3)} \quad (3.91)$$

may be precomputed.Using these pre-computed quantities for each element, equation (3.89) may be rewritten as:

$$\int_{\Omega} M_{is} M_{jt} d\Omega = \Delta \sum_{p=1}^{3} \sum_{q=1}^{3} U_1(i,j,p,q) \frac{\partial \zeta_p}{\partial s} \frac{\partial \zeta_q}{\partial t}, \quad (3.92)$$

[5]By this we mean compute everything that is independent of geometry and materials.

and similarly, equation (3.87) may be rewritten as:

$$\int_{\Omega} \alpha_i M_{js} d\Omega = \Delta \sum_{p=1}^{3} U_2(i,j,p) \frac{\partial \zeta_p}{\partial s}. \tag{3.93}$$

So the complete expression for equation (3.68) is defined by the integral of each of the components of the matrix:

$$\int_{\Omega} \Gamma_{11} d\Omega = \Delta \beta^2 T_{ij}^{(3)} + \sum_{p=1}^{3} \sum_{q=1}^{3} U_1(i,j,p,q) \frac{\partial \zeta_p}{\partial y} \frac{\partial \zeta_q}{\partial y}, \tag{3.94}$$

$$\int_{\Omega} \Gamma_{12} d\Omega = -\Delta \sum_{p=1}^{3} \sum_{q=1}^{3} U_1(i,j,p,q) \frac{\partial \zeta_p}{\partial y} \frac{\partial \zeta_q}{\partial x}, \tag{3.95}$$

$$\int_{\Omega} \Gamma_{13} d\Omega = \Delta \beta \sum_{p=1}^{3} U_2(i,j,p) \frac{\partial \zeta_p}{\partial x}, \tag{3.96}$$

$$\int_{\Omega} \Gamma_{21} d\Omega = -\Delta \sum_{p=1}^{3} \sum_{q=1}^{3} U_1(i,j,p,q) \frac{\partial \zeta_p}{\partial x} \frac{\partial \zeta_q}{\partial y}, \tag{3.97}$$

$$\int_{\Omega} \Gamma_{22} d\Omega = \Delta \sum_{p=1}^{3} \sum_{q=1}^{3} U_1(i,j,p,q) \frac{\partial \zeta_p}{\partial x} \frac{\partial \zeta_q}{\partial x} + \Delta \beta^2 T_{ij}^{(3)}, \tag{3.98}$$

$$\int_{\Omega} \Gamma_{23} d\Omega = \Delta \beta \sum_{p=1}^{3} U_2(i,j,p) \frac{\partial \zeta_p}{\partial y}, \tag{3.99}$$

$$\int_{\Omega} \Gamma_{31} d\Omega = \Delta \beta \sum_{p=1}^{3} U_2(i,j,p) \frac{\partial \zeta_p}{\partial x}, \tag{3.100}$$

$$\int_{\Omega} \Gamma_{32} d\Omega = \Delta\beta \sum_{p=1}^{3} U_2(i,j,p) \frac{\partial \zeta_p}{\partial y}, \tag{3.101}$$

$$\int_{\Omega} \Gamma_{33} d\Omega = \Delta \sum_{p=1}^{3} \sum_{q=1}^{3} U_1(i,j,p,q) \frac{\partial \zeta_p}{\partial x} \frac{\partial \zeta_q}{\partial x}$$

$$+ \Delta \sum_{p=1}^{3} \sum_{q=1}^{3} U_1(i,j,p,q) \frac{\partial \zeta_p}{\partial y} \frac{\partial \zeta_q}{\partial y}. \tag{3.102}$$

3.3.2 The N Matrix

From (3.58) and (3.54) through (3.56), the N matrix is completely defined by:

$$\mathbf{N} = \begin{pmatrix} \Upsilon_{11} & \Upsilon_{12} & \Upsilon_{13} \\ \Upsilon_{21} & \Upsilon_{22} & \Upsilon_{23} \\ \Upsilon_{31} & \Upsilon_{32} & \Upsilon_{33} \end{pmatrix} \tag{3.103}$$

where:

$$\Upsilon_{mn} = \alpha_i \alpha_j \quad \text{for } m = n \tag{3.104}$$

$$\Upsilon_{mn} = 0 \quad \text{for } m \neq n. \tag{3.105}$$

Previously we found that

$$\int_{\Omega} \alpha_i \alpha_j d\Omega = \Delta T_{ij}^{(3)}. \tag{3.106}$$

Therefore the N matrix is completely defined by:

$$\int_{\Omega} \mathbf{N} d\Omega = \Delta \begin{pmatrix} \mathrm{T}_{ij}^{(3)} & 0 & 0 \\ 0 & \mathrm{T}_{ij}^{(3)} & 0 \\ 0 & 0 & \mathrm{T}_{ij}^{(3)} \end{pmatrix}. \tag{3.107}$$

3.3.3 The P matrix

From (3.66) and (3.62) through (3.64), the matrix P is completely defined by:

$$\mathbf{P} = \begin{pmatrix} \Xi_{11} & \Xi_{12} & \Xi_{13} \\ \Xi_{21} & \Xi_{22} & \Xi_{23} \\ \Xi_{31} & \Xi_{32} & \Xi_{33} \end{pmatrix} \tag{3.108}$$

where:

$$\Xi_{11} = M_{xi} M_{xj} \tag{3.109}$$

$$\Xi_{12} = M_{xi} M_{yj} \tag{3.110}$$

$$\Xi_{13} = -\beta \alpha_j M_{xi} \tag{3.111}$$

$$\Xi_{21} = M_{yi} M_{xj} \tag{3.112}$$

$$\Xi_{22} = M_{yi} M_{yj} \tag{3.113}$$

$$\Xi_{23} = -\beta \alpha_j M_{yi} \tag{3.114}$$

$$\Xi_{31} = -\beta \alpha_i M_{xj} \tag{3.115}$$

$$\Xi_{32} = -\beta \alpha_i M_{yj} \tag{3.116}$$

$$\Xi_{33} = \beta^2 \alpha_i \alpha_j \tag{3.117}$$

Examining equations (3.109) through (3.117) reveals three common expressions defined in equations (3.78) through (3.80). Using those results, equation (3.108) is completely defined by the integral of each of it's components:

$$\int_\Omega \Xi_{11} d\Omega = \Delta \sum_{p=1}^{3} \sum_{q=1}^{3} U_1(i,j,p,q) \frac{\partial \zeta_p}{\partial x} \frac{\partial \zeta_q}{\partial x}, \tag{3.118}$$

$$\int_\Omega \Xi_{12} d\Omega = \Delta \sum_{p=1}^{3} \sum_{q=1}^{3} U_1(i,j,p,q) \frac{\partial \zeta_p}{\partial x} \frac{\partial \zeta_q}{\partial y}, \tag{3.119}$$

$$\int_\Omega \Xi_{13} d\Omega = -\Delta \beta \sum_{p=1}^{3} U_2(i,j,p) \frac{\partial \zeta_p}{\partial x}, \tag{3.120}$$

$$\int_\Omega \Xi_{21} d\Omega = \Delta \sum_{p=1}^{3} \sum_{q=1}^{3} U_1(i,j,p,q) \frac{\partial \zeta_p}{\partial y} \frac{\partial \zeta_q}{\partial x}, \tag{3.121}$$

$$\int_\Omega \Xi_{22} d\Omega = \Delta \sum_{p=1}^{3} \sum_{q=1}^{3} U_1(i,j,p,q) \frac{\partial \zeta_p}{\partial y} \frac{\partial \zeta_q}{\partial y}, \tag{3.122}$$

$$\int_\Omega \Xi_{23} d\Omega = -\Delta \beta \sum_{p=1}^{3} U_2(i,j,p) \frac{\partial \zeta_p}{\partial y}, \tag{3.123}$$

$$\int_\Omega \Xi_{31} d\Omega = -\Delta \beta \sum_{p=1}^{3} U_2(i,j,p) \frac{\partial \zeta_p}{\partial x}, \tag{3.124}$$

$$\int_{\Omega} \Xi_{32} d\Omega = -\Delta\beta \sum_{p=1}^{3} U_2(i,j,p) \frac{\partial \zeta_p}{\partial y}, \tag{3.125}$$

$$\int_{\Omega} \Xi_{33} d\Omega = \Delta\beta^2 T_{ij}^{(3)}. \tag{3.126}$$

3.4 Making use of the matrix expressions

Having derived third order finite element expressions for the required functional we are left with implementing these expressions in a finite element program. There is nothing inherently difficult about this provided appropriate data structures are selected.

Boundary conditions are imposed by fixing appropriate nodal values. In addition, boundaries are not required to line up with the coordinate axes. Interface conditions are met by matching nodal values at inter-element boundaries.

The m solutions of equation (3.8) with $k^2 = 0$ form a basis for the divergence-free subspace. By restricting the trial functions of (3.7) according to

$$\mathbf{x} = \mathbf{Q}\mathbf{y} \tag{3.127}$$

where $\mathbf{Q}$ is an $n \times m$ matrix whose columns are the m solutions of (3.8) and $\mathbf{y}$ is an $m \times 1$ column vector, $\mathbf{x}$ will necessarily be divergence-free and will satisfy the essential boundary conditions. Substituting (3.127) into (3.7)

yields a reduced $m \times m$ eigenvalue problem of the form:

$$\mathbf{Q}^t\mathbf{A}\mathbf{Q}\mathbf{y} = k^2\mathbf{Q}^t\mathbf{B}\mathbf{Q}\mathbf{y}. \tag{3.128}$$

This we recognize as a classical eigenvalue problem which may be solved using any of several prepackaged eigenvalue solvers[6]. Having found the solutions $\mathbf{y}$, we may compute the $\mathbf{x}$'s by equation (3.127).

3.5 Summary

In this chapter the required functional was transformed into a third order finite element implementation. It was implicitly shown how the matrix expressions may be represented in a computer program. By restricting the trial functions to a solenoidal sub-space satisfying the original boundary conditions of the problem it was shown how divergence-free solutions may be obtained.

We are not restricted to computing the divergence-free trial functions in the manner shown in this chapter. It was shown that the divergence-free trial functions are represented by a matrix $\mathbf{Q}$ and in general, $\mathbf{Q}$ may be determined by whatever means are available.

In the next chapter, three case studies of waveguide structures analyzed

[6]Sparsity issues aside, there exist several commercially available eigensolvers. As will be shown in chapter 4, sparsity plays an important role in how we solve the eigenvalue problem.

are presented that make use of this finite element implementation.

Chapter 4

Results

In the previous chapters a method was presented which generates divergence-free basis vectors from the original problem formulation and using these basis vectors, computes the correct modes of the waveguide. In this chapter, three case studies of waveguide structures are presented.

Each case study in this chapter increases in complexity from a hollow rectangular waveguide to a block-loaded rectangular waveguide. The finite element models are identical for each with only the material selection varying from one example to the next.

Data pertaining to the actual modes obtained versus analytical results are presented wherever possible. Other data such as the number of trial functions required for the generation of the divergence-free bases and the number of divergence-free bases actually computed are presented. In addition, data

relating sparsity of the resulting assembly matrices is presented.

The chapter concludes with general observations and remarks regarding the solutions to each of the problems.

4.1 Simple rectangular waveguide

4.1.1 Geometry

Consider a rectangular waveguide of dimension 1 meter wide and 0.6 meters high, completely clad with a good conductor. The waveguide possesses longitudinal symmetry and so we can model the waveguide in the cross-section. The waveguide may be represented by 16 third-order triangular elements as depicted in Figure 4.1. Neumann[1] boundary conditions are used to model the conductor. The propagation constant, β, is set equal to zero.

The purpose of this experiment is to extract the correct modes of the waveguide, for which analytical results are available, and to ascertain the validity of the method, at least insofar as simple rectangular waveguides are concerned.

[1] A Neumann boundary condition dictates that the field must be tangential to the surface at which the constraint is defined. See equation (2.47).

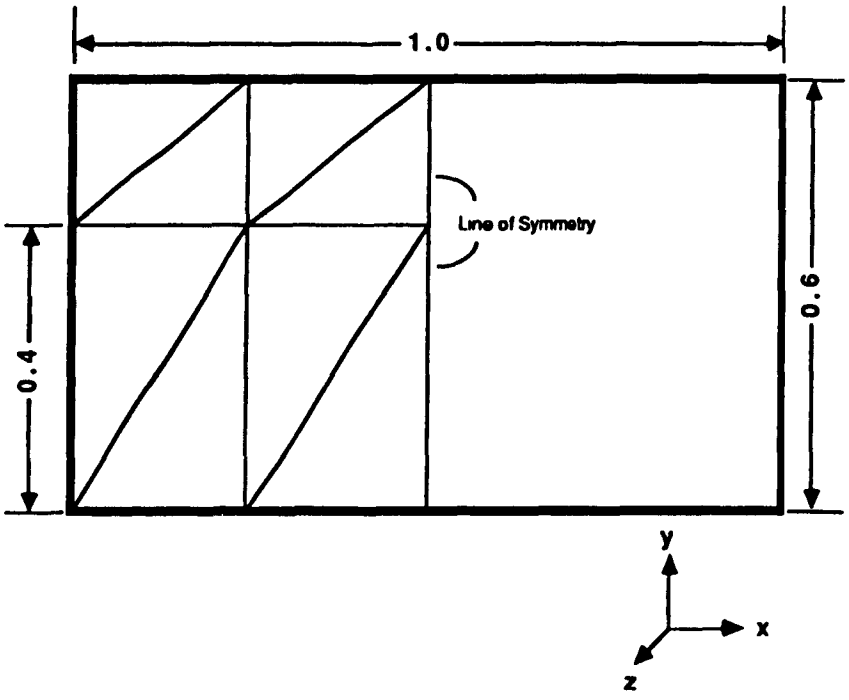

Figure 4.1: A hollow reactangular waveguide

This figure depicts the finite element model of a hollow rectangular waveguide. A line of symmetry delineates the half problem which may be solved.

4.1.2 Method

For problems exhibiting symmetry, only half the problem need be solved. The line of symmetry is taken care of by first solving the problem with the line of symmetry constrained to Neumann boundary conditions and then resolving with the line of symmetry constrained to Dirichlet[2] boundary conditions. Admittedly there is not much to gain in taking advantage of symmetry for such a small scale problem, but in general, symmetry conditions should be taken advantage of wherever possible.[3]

Solving the problem twice produces two sets of solutions which are merged to hopefully yield the same solution as if the problem were solved once for the complete geometry.

4.1.3 Results

The initial solution corresponding to a waveguide with Neumann boundary conditions along the line of symmetry produced global assembly matrices

[2]A Dirichlet boundary condition dictates that the field must be normal to the surface at which the constraint is defined. See equation (2.11).

[3]Taking advantage of symmetry compensates for memory constraints on the computer, since only half the geometry need be represented. In addition, because the problems are typically solved in $O(n^3)$ time, solving a problem twice as big takes eight times longer. Using symmetry, solving the problem twice, in general, takes only twice as long.

of dimension 119×119 containing 2140[4] non-zero entries. A total of 72 zero-eigenvalues, corresponding to divergence-free trial functions were found. Using the trial functions, reduced global assembly matrices of dimension 72×72 were created requiring 2628 non-zero entries.

The solution corresponding to a waveguide having Dirichlet boundary condition along the line of symmetry produced global assembly matrices of dimension 114×114 containing 1998 non-zero entries. A total of 66 zero-eigenvalues were found. Using the divergence-free trial functions, reduced global assembly matrices of dimension 66×66 were created requiring 2211 non-zero entries.

The first six computed modes are accurate to within 0.3% of the analytical results. Refer to Table 4.2 for a detailed list of results.

A variation to the above problem where the material inside the guide has a relative permittivity, ε, of 6 was solved. Identical results were produced with respect to the number of divergence-free basis vectors generated and the number of non-zero entries in the global assembly matrices. The results are depicted in Table 4.3. Again, for the first six modes computed, results obtained were within 0.3% of the analytical results.

[4]Figures quoted assume the matrices are stored in full. In practice, only the lower triangle requires storage.

	Neumann		Dirichlet	
	Pass-1	Pass-2	Pass-1	Pass-2
Degrees of Freedom	119	72	114	66
Non-zero's	2140	2628	1998	2211
% Full	15.1	50.7	15.4	50.7
% Reduction	-	+22.8%	-	+10.6%

Table 4.1: Summary of sparsity results for a simple rectangular waveguide.

This table summarizes the sparsity results obtained for a simple rectangular waveguide. Identical results were obtained for $\epsilon = 1$ ***and*** $\epsilon = 6$. ***The row labeled Degrees of Freedom indicates the dimension of the*** $m \times m$ ***assembly matrices. The row labeled Non-zeros indicates the number of non-zero entries in the assembly matrices. The row labeled % Full indicates the percentage of entries in the assembly matrices that are non-zero. The row labeled % Reduction indicates the percentage increase(decrease) in the number of non-zero entries from Pass-1 to Pass-2.***

β	Mode	k_o^2-FEM	Normalized	Analytic	% Error
0.00	10	9.8695	1.0000	1.0000	0.00
	01	27.421	2.7784	2.7778	0.01
	11	37.337	3.7831	3.7778	0.14
	20	39.482	4.0004	4.0000	0.01
	21	67.095	6.7981	6.7778	0.29
	30	88.928	9.0103	9.0000	0.11
	02	110.74	11.220	11.111	0.98
	31	117.45	11.901	11.777	1.05
	12	120.72	12.231	12.111	0.99
	22	153.89	15.592	15.111	3.18
	40	158.00	16.008	16.000	0.05
	41	189.43	19.193	18.777	2.21
	32	205.55	20.826	20.111	3.55
	03	251.06	25.437	25.000	1.74

Table 4.2: Results for an empty rectangular waveguide with $\beta = 0$ and $\epsilon_r = 1$.

The first 14 modes produced by the proposed method, for a hollow rectangular waveguide. No spurious modes were encountered.

β	Mode	k_o^2-FEM	Normalized	Analytic	% Error
0.00	10	1.6449	0.1666	0.1666	0.00
	01	4.5702	0.4630	0.4630	0.00
	11	6.2229	0.6305	0.6296	0.14
	20	6.5804	0.6667	0.6666	0.01
	21	11.182	1.1330	1.1296	0.30
	30	14.821	1.5017	1.5000	0.11
	02	18.457	1.8701	1.8518	0.98
	31	19.576	1.9835	1.9630	1.04
	12	20.120	2.0386	2.0185	0.99
	22	25.648	2.5987	2.5185	3.18
	40	26.333	2.6681	2.6667	0.05
	41	31.572	3.1989	3.1296	2.21
	32	34.258	3.4711	3.3518	3.55
	03	41.843	4.2396	4.1666	1.75

Table 4.3: Results for a completely filled rectangular waveguide with $\beta = 0$ and $\epsilon_r = 6$.

The first 14 modes produced by the proposed method for a simple rectangular waveguide completely filled with dielectric.

4.2 Slab-loaded rectangular waveguide

4.2.1 Geometry

Consider the same waveguide described above but this time slab-loaded with dielectric having relative permittivity, $\varepsilon = 6$. The waveguide is solved with a range of propagation constants varying from $\beta = 0$ to $\beta = 4$, in increments of 1.

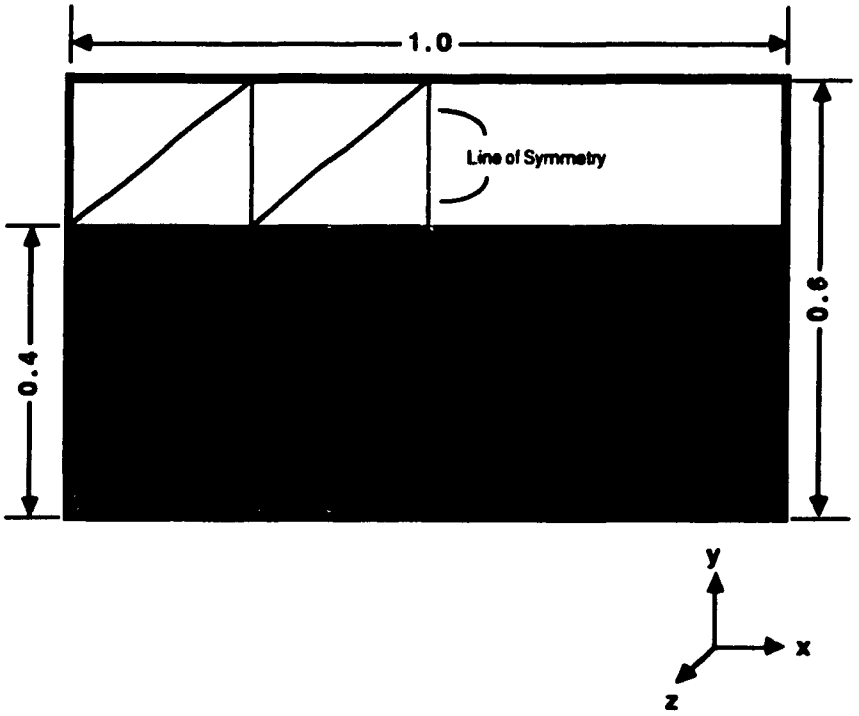

Figure 4.2: A slab-loaded rectangular waveguide

This figure depicts the finite element model of a slab-loaded rectangular waveguide. The dielectric is assumed to have an $\varepsilon = 6$.

4.2.2 Method

As was previously the case, two sets of modes are produced for each symmetric contribution. A total of ten solutions were generated: five for each of the propagation constants and that for each symmetric contribution.

4.2.3 Results

The initial solution corresponding to a waveguide with Neumann boundary conditions along the line of symmetry produced global assembly matrices of dimension 119×119, containing 2140 non-zero entries. A total of 72 zero-eigenvalues were computed yielding assembly matrices of dimension 72×72, containing 2628 non-zero entries.

The solution corresponding to a waveguide with Dirichlet boundary condition along the line of symmetry produced global assembly matrices of dimension 114×114, containing 1998 non-zero entries. A total of 66 zero-eigenvalues were computed yielding assembly matrices of dimension 66×66, containing 2211 non-zero entries.

For $\beta > 0$, the solutions with Neumann boundary conditions along the line of symmetry produced global assembly matrices of dimension 47×47 containing 1128 non-zero entries. The solutions with Dirichlet boundary conditions along the line of symmetry produced global assembly matrices of dimension 44×44 containing 990 non-zero entries.

	Neumann			Dirichlet		
	Pass-1	Pass-2 $\beta = 0$	Pass-2 $\beta > 0$	Pass-1	Pass-2 $\beta = 0$	Pass-2 $\beta > 0$
Degrees of Freedom	119	72	47	114	66	44
Non-zero's	2140	2628	1128	1998	2211	990
% Full	15.1%	50.7%	51.1%	15.4%	50.7%	51.1%
% Reduction	-	(22.8%)	47%	-	(10.6%)	50.5%

Table 4.4: Summary of sparsity results for a slab-loaded rectangular waveguide

This table lists the sparsity results obtained for the solution of a slab-loaded rectangular waveguide.

The results are depicted in Table 4.3. Analytical results were extracted from [47]. and are listed next to the computed results.

4.3 Block-Loaded Rectangular Waveguide

4.3.1 Geometry

The same waveguide structure as in the previous example is solved for repeatedly with propagation constants varying from β equal to 0 to 4, in increments of 1. The waveguide is assumed to be be block-loaded with a material having a relative permittivity of 6.

4.3.2 Method

Two sets of modes are produced for each of the five possible propagation constants. The solutions are merged to yield the complete solution.

4.3.3 Results

Identical sparsity results, with respect to the slab-loaded waveguide problem, were obtained. See Table 4.4. The results are listed in Table 4.5. Analytical results were unavailable for this problem.

β	Mode	k_o–FEM	k_o–Analytic	% Error
0.00	1	1.7667	1.7666	0.01
	2	2.3056	2.3053	0.01
	3	2.6853	2.6779	0.28
	4	2.9568	2.9548	0.07
	5	3.3036	3.2987	0.15
	6	3.5853	3.5524	0.93
	7	4.1549	4.1380	0.41
1.00	1	1.8412	1.8310	0.60
	2	2.3873	2.3460	1.80
	3	2.7273	2.7125	0.50
	4	3.0284	2.9842	1.50
	5	3.4926	3.3874	3.10
	6	3.6150	3.5777	1.00
	7	4.2359	4.1584	1.90
2.00	1	2.0048	2.0000	0.20
	2	2.4998	2.4637	1.50
	3	2.8265	2.8137	0.50
	4	3.1078	3.0699	1.20
	5	3.7415	3.6363	2.90
	6	3.6892	3.6528	1.00
	7	4.2911	4.2187	1.70
3.00	1	2.2411	2.2383	0.10
	2	2.6782	2.6473	1.20
	3	2.9891	2.9739	0.50
	4	3.2418	3.2071	1.10
	5	3.8132	3.7774	0.90
	6	4.1204	3.9951	3.10
	7	4.3872	4.3172	1.60
4.00	1	2.5154	2.5138	0.10
	2	2.9105	2.8832	0.90
	3	3.2000	3.1835	0.50
	4	3.4194	3.3886	0.90
	5	3.9790	3.9376	1.10
	6	4.5013	4.3941	2.40
	7	4.5721	4.4513	2.70

Figure 4.3: Results for a slab-loaded rectangular waveguide

This table lists the first 7 modes produced by the proposed method, for a slab loaded rectangular waveguide filled with material having relative permittivity of 6. The units are $\beta(rad/m)$, $k_o(rad/m)$.

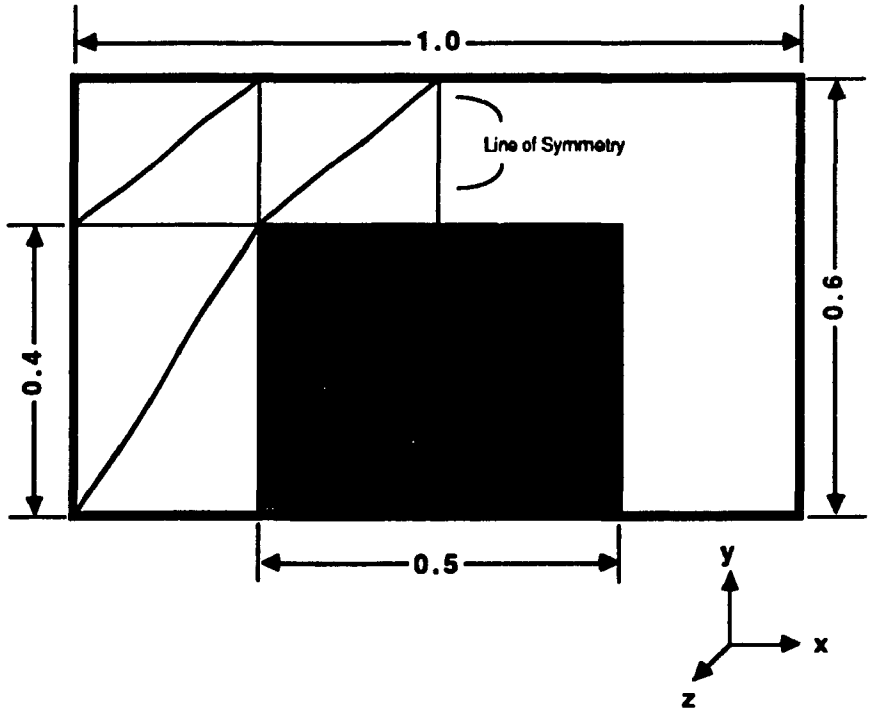

Figure 4.4: A block-loaded rectangular waveguide

This figure depicts the finite element model of a block-loaded rectangular waveguide.

β	Mode	k_o^2-FEM	Normalized ($\times\pi^2$)
0.00	1	4.1488	0.4203
	2	8.2942	0.8403
	3	10.009	1.0141
	4	17.541	1.7773
	5	19.228	1.9482
	6	24.541	2.4865
	7	34.029	3.4479
1.00	1	4.4490	0.4507
	2	9.0065	0.9184
	3	10.866	1.1009
	4	17.798	1.8033
	5	20.810	2.1085
	6	26.544	2.6895
	7	36.637	3.7121
2.00	1	5.0801	0.5147
	2	11.073	1.1220
	3	11.592	1.1745
	4	19.110	1.9362
	5	27.436	2.7798
	6	28.083	2.8454
	7	37.400	3.7895
3.00	1	6.1146	0.6195
	2	13.501	1.3679
	3	14.495	1.4687
	4	18.091	1.8331
	5	27.837	2.8205
	6	30.336	3.0736
	7	38.437	3.8945
4.00	1	7.4833	0.7582
	2	14.261	1.4449
	3	19.039	1.9291
	4	19.182	1.9435
	5	32.540	3.2970
	6	33.074	3.3511
	7	40.149	4.0679

Figure 4.5: Results for a block-loaded rectangular waveguide with $\beta = 0$.

This table lists the first 7 modes produced by the proposed method, for a block-loaded rectangular waveguide filled with material having relative permittivity of 6.

Chapter 5

Conclusion

Several observations can be made from the results generated in chapter 4:

- No spurious modes are produced with this method.
- For $\beta > 0$, the number of non-zeroes in the reduced (step 2) matrices is less than in the original (step 1) matrices.
- The dimension of the reduced assembly matrices is considerably smaller than the dimension of the original matrices.

The fact that no spurious modes are produced stems directly from the reduced set of trial functions used in step 2 of the method. Solutions with non-zero divergence cannot be produced since the trial functions themselves are divergence-free. By imposing the non-divergence constraint throughout

the region of the problem, we achieve the desired goal of generating only those solutions which are solenoidal.

The fact that the number of non-zero entries decreased for cases when $\beta > 0$, is a result of the reduced dimension of the matrices. In general, we cannot say anything about the number of non-zeroes in the reduced matrices. The apparent savings are probably coincidental. Since the trial functions are defined throughout the region of the problem , we expect that the reduced matrices would be full. This is to be compared to the *Penalty Method* which produces matrices which are inherently sparse.

The dimensions of the global matrices are a function of the number of divergence-free trial functions defined in the solution space. Other workers report that, for three dimensional problems, the *Reduction Method* produces matrices approximately one-third the size of matrices conventionally produced with the *Penalty Method.*[1] Not enough evidence exists to draw a relationship to two dimensional problems. More complex waveguide structures would have to be studied in order to verify this claim.

What does this mean practically? Large eigenvalue problems are traditionally solved using sparse-matrix techniques. Sparse-matrix eigenvalue solvers can typically do better than $O(n^3)$ time[2]. The solver used in this thesis[3] could produce the lowest p eigenvectors in $O(n^2)$. While this indi-

[1] See [46].

[2] n is the order of the matrix being solved for.

[3] A sparse solver was used since it was the only one available at the time. In addition, due to the way the divergence-free trial functions were computed, it did not make sense

cates that the *Reduction Method* is superior to the *Penalty Method* for small problems, large eigenvalue problems are less efficiently solved. In addition, the method used to compute divergence-free trial functions in this thesis is far from ideal. Other, more efficient methods need to be developed. Ideally, the assembly matrices produced by the proposed method would be sparse, and hence all the benefits of the *Penalty Method* would immediately be inherited. To date, nobody has shown how to construct sparse assembly matrices having divergence-free properties.

Future Work

Results of this research have certainly made apparent other avenues of research.

Although the problems solved in this thesis could be solved in the cross-section, more complicated structures such as cavity resonators cannot. An obvious extension to this work would be to adapt the method to three dimensions. In addition, the method could be adapted to solve problems having lossy, anisotropic materials.

Finally, the general problem of computing sparse matrices having divergence-free properties certainly deserves more attention.

---

to have two separate solvers incorporated in the software.

Bibliography

[1] W.L. Barrow, "Transmission of Electromagnetic Waves in Hollow Tubes of Metal," *Proc. of the Institute of Radio Engineers*, vol. 24, pp. 1298–1328, October 1936.

[2] A.D. Berk, "Variational Principles for Electromagnetic Resonators and Waveguides," *IRE Trans. on Antennas and Propagation*, vol. , pp. 104–111, April 1956.

[3] S. Ahmed, "Finite-Element Method for Waveguide Problems," *Electronics Letters*, vol. 4, No. 18, pp. 387–389, September 1968.

[4] P. Silvester, "A General High-Order Finite-Element Waveguide Analysis Program," *IEEE Trans. on Microwave Theory and Techniques*, vol. MTT-17, pp. 204–210, April 1969.

[5] P. Silvester, "High-Order Polynomial Triangular Finite Elements for Potential Problems," *Int J. Engng. Sci.*, vol. 7, pp. 849–861, 1969.

[6] S. Ahmed, P. Daly, "Finite-element methods for inhomogeneous waveguides," *Proc. IEE*, vol. 116, No. 10, pp. 1661–1664, October 1969.

[7] Zoltan J. Csendes, P. Silvester, "Numerical Solution of Dielectric Loaded Waveguides: I–Finite- Element Analysis," *IEEE Trans. on Microwave Theory and Techniques*, vol. MTT-18, No. 12, pp. 1124–1131, December 1970.

[8] P. Daly, "Hybrid-Mode Analysis of Microstrip by Finite-Element Methods," *IEEE Trans. on Microwave Theory and Techniques*, vol. MTT-19, No. 1, pp. 19–25, January 1971.

[9] P. Silvester, "Tetrahedral Polynomial Finite Elements For the Helmholtz Equation," *Int J. Num. Meth. Engng*, vol. 4, pp. 405–413, 1972.

[10] Douglas G. Corr, J. Brian Davies, "Computer Analysis of the Fundamental and Higher Order Modes in Single and Coupled Microstrip," *IEEE Trans. on Microwave Theory and Techniques*, vol. MTT-20, No. 10, pp. 669–678, October 1972.

[11] C.G. Williams, G.K. Cambrell, "Numerical Solution of Surface Waveguide Modes Using Transverse Field Components," *IEEE Trans. on Microwave Theory and Techniques*, vol. MTT-21, No. 3, pp. 329–330, March 1974.

[12] M. Albani, P. Bernardi, "A Numerical Method Based on the Discretization of Maxwell Equations in Integral Form," *IEEE Trans. on Microwave Theory and Techniques*, vol. MTT-21, No. 4, pp. 446–450, April 1974.

[13] S. Akhtarzad, P.B. Johns, "Solution of Maxwell's equations in three space dimensions and time by the t.l.m method of numrical analysis.," *Proc. IEE*, vol. 122, No. 12, pp. 1344–1348, December 1975.

[14] C. Yeh, S.B. Dong, W. Oliver, "Arbitrarily shaped inhomogeneous optical fiber or integrated optical waveguides," *Journal of Applied Physics*, vol. 46, No. 5, pp. 2125–2129, May 1975.

[15] A. Konrad, "Vector Variational Formulation of Electromagnetic Fields in Anisotropic Media," *IEEE Trans. on Microwave Theory and Techniques*, vol. MTT-24, No. 9, pp. 553–559, September 1976.

[16] P. Vandenbulke, P.E. Lagasse, "Eigenmode Analysis of Anisotropic Optical Fibres or Integrated Optical Waveguides," *Electronics Letters*, vol. 12, No. 5, pp. 120–122, March 1976.

[17] A. Konrad, "High-Order Triangular Finite Elements for Electromagnetic Waves in Anisotropic Media," *IEEE Trans. on Microwave Theory and Techniques*, vol. MTT-25, No. 5, pp. 353–360, May 1977.

[18] T.S. Bird, "Propagation and Radiation Characteristics of Rib Waveguides," *Electronics Letters*, vol. 13, No. 14, pp. 401–403, July 1977.

[19] P. Silvester, "Construction of Triangular Finite Element Universal Matrices," *Int J. Num. Meth. Engng*, vol. 12, pp. 237–244, 1978.

[20] Theodore G. Mihran, "Microwave Oven Mode Tuning by Slab Dielectric Loads," *IEEE Trans. on Microwave Theory and Techniques*, vol. MTT-26, No. 6, pp. 381–387, June 1978.

[21] R.L. Ferrari, G.L. Maile, "Three Dimensional Finite Element Method for Solving Electromagnetic Problems," *Electronics Letters*, vol. 14, No. 15, pp. 467–468, July 1978.

[22] N. Mabaya, P.E. Lagasse, and P. Vandenbulke, "Finite Element Analysis of Optical Waveguides," *IEEE Trans. on Microwave Theory and Techniques*, vol. MTT-29, No. 6, pp. 600–605, June 1981.

[23] Masatoshi Ikeuchi, Hideo Sawami, Hiroshi Niki, "Analysis of Open-Type Dielectric Waveguides by the Finite-Element Iterative Method," *IEEE Trans. on Microwave Theory and Techniques*, vol. MTT-29, No. 3, pp. 234–239, March 1981.

[24] Mansonori Koshiba, Kazuya Hayata, Michio Suzuki, "Approximate Scalar Finite-Element Analysis of Anisotropic Optical Waveguides.," *Electronics Letters*, vol. ??, No. ??, pp. ???–???, March 1982.

[25] P. Silvester, "Universal Finite Element Matrices for Tetrahedra," *Int J. Num. Meth. Engng*, vol. 18, pp. 1055–1061, 1982.

[26] S.J. Fiedziuszko, "Dual-Mode Dielectric Resonator Loaded Cavity Filters," *IEEE Trans. on Microwave Theory and Techniques*, vol. MTT-30, No. 9, pp. 1311–1316, September 1982.

[27] J. Brian Davies, F. Anibal Fernandez, Glafkos Y. Philippou, "Finite Element Analysis of all Modes in Cavities with Circular Symmetry," *IEEE Trans. on Microwave Theory and Techniques*, vol. MTT-30, No. 11, pp. 1975–1980, November 1982.

[28] A. Konrad, "Three-dimensional finite element solution of anisotropic complex potential problems," *Journal of Applied Physics*, vol. 53, No.11, pp. 8408–8410, November 1982.

[29] Karl Gustafson, Robert Hartman, "Divergence-Free Bases for Finite Element Schemes in Hydrodynamics," *SIAM Journal of Numerical Analysis*, vol. 20, pp. 697–721, August 1983.

[30] J.P. Webb, G.L. Maile, and R.L. Ferrari, "Finite-element solution of three-dimensional electromagnetic problems," *Proc. IEE*, vol. 130. Pt H, No. 2, pp. 153–158, March 1983.

[31] M. Hara, T. Wada, T. Fukasawa, F. Kikuchi, "A Three Dimensional Analysis of RF Electromagnetic Fields By The Finite-Element Method," *IEEE Trans. on Magnetics*, vol. MAG-19, No. 6, pp. 2417–2420, November 1983.

[32] Mansonori Koshiba, Kazuya Hayata, Michio Suzuki, "Vectorial Finite-Element Method Without Spurious Solutions For Dielectric Waveguide Problems," *Electronics Letters*, vol. 20, No. 10, pp. 409–410, May 1984.

[33] Mansonori Koshiba, Kazuya Hayata, Michio Suzuki, "Approximate Scalar Finite-Element Analysis of Anisotropic Optical Waveguides with Off-Diagonal Elements in a Permittivity Tensor," *IEEE Trans. on Microwave Theory and Techniques*, vol. MTT-32, No. 6, pp. 587–593, June 1984.

[34] Mitsuo Hano, "Finite-Element Analysis of Dielectric-Loaded Waveguides," *IEEE Trans. on Microwave Theory and Techniques*, vol. MTT-32, No. 10, pp. 1275–1279, October 1984.

[35] B.M. Azizur Rahman, J. Brian Davies, "Finite-Element Analysis of Optical and Microwave Waveguide Problems," *IEEE Trans. on Microwave Theory and Techniques*, vol. MTT-32, No. 1, pp. 20–28, January 1984.

[36] B.M. Azizur Rahman, J. Brian Davies, "Penalty Function Improvement of Waveguide Solution by Finite Elements," *IEEE Trans. on Microwave Theory and Techniques*, vol. MTT-32, No. 8, pp. 922–928, August 1984.

[37] N. Nassif, "Vector Interpolation Polynomials over Finite Elements," McGill University Ph.D. Thesis, September 1984.

[38] A. Konrad, "A Direct Three-Dimensional Finite Element Method For The Solution of Electromagnetic Fields in Cavities," *IEEE Trans. on Magnetics*, vol. MAG-33, No. 6, pp. 2276–2279, November 1985.

[39] Daniel Welt, Jon Webb, "Finite-Element Analysis of Dielectric Waveguides with Curved Boundaries," *IEEE Trans. on Microwave Theory and Techniques*, vol. MTT-33, No. 7, pp. 576–585, July 1985.

[40] Ruey-Beei Wu, Chun Hsiung Chen, "On the Variational Reaction Theory for Dielectric Waveguides," *IEEE Trans. on Microwave Theory and Techniques*, vol. MTT-33, No. 6, pp. 477–483, June 1985.

[41] J.P. Webb, "The Finite-Element Method for Finding Modes of Dielectric-Loaded Cavities," *IEEE Trans. on Microwave Theory and Techniques*, vol. MTT-33, No. 7, pp. 635–639, July 1985.

[42] A. Konrad, "On the Reduction of the Number of Spurious Modes in the Vectorial Finite-Element Solution of Three-Dimensional Cavities and Waveguides," *IEEE Trans. on Microwave Theory and Techniques*, vol. MTT-34, No. 2, pp. 224–227, February 1986.

[43] A.J. Kobelansky, J.P. Webb, "Eliminating Spurious Modes in Finite Element Waveguide Problems by using Divergence-Free Fields," *Electronics Letters*, vol. 22, No. 11, pp. 569–570, May 1986.

[44] K. Hayata, M. Koshiba, M. Eguchi, M. Suzuki, "Vectorial Finite-Element Method Without Any Spurious Solutions for Dielectric Waveguiding Problems Using transverse Magnetic-Field Component," *IEEE Trans. on Microwave Theory and Techniques*, vol. MTT-34, No. 11, pp. 1120–1124, November 1986.

[45] C.W. Crowley, P.P. Silvester, H. Hurwitz Jr., "Covariant Projection Elements for 3D Vector Field Problems," *IEEE Trans. on Magnetics*, vol. MAG-24, No. 1, pp. 397–400, January 1988.

[46] J.P. Webb, "Efficient Generation of Divergence-Free Fields For the Finite Element Analysis of 3D Cavity Resonators," *IEEE Trans. on Magnetics*, vol. MAG-24, No. 1, pp. 162–165, January 1988.

[47] L. Young, *Advances in Microwaves, Vol. 1.* London: Academic Press, 1966.